

Medium effects in antikaon-induced Ξ^- hyperon production on nuclei near threshold

E. Ya. Paryev^{1,2}

¹*Institute for Nuclear Research, Russian Academy of Sciences,
Moscow 117312, Russia*

²*Institute for Theoretical and Experimental Physics,
Moscow 117218, Russia*

Abstract

We study the antikaon-induced inclusive cascade Ξ^- hyperon production from ^{12}C and ^{184}W target nuclei near threshold within a nuclear spectral function approach. The approach describes incoherent direct Ξ^- hyperon production in elementary $K^-p \rightarrow K^+\Xi^-$ and $K^-n \rightarrow K^0\Xi^-$ processes as well as takes into account the influence of the scalar nuclear K^-, K^+, K^0, Ξ^- and their Coulomb potentials on these processes. We calculate the absolute differential and total cross sections for the production of Ξ^- hyperons off these nuclei at laboratory angles $\leq 45^\circ$ by K^- mesons with momenta of 1.0 and 1.3 GeV/c, which are close to the threshold momentum (1.05 GeV/c) for Ξ^- hyperon production on the free target nucleon at rest. We also calculate the momentum dependence of the transparency ratio for the $^{184}\text{W}/^{12}\text{C}$ combination for Ξ^- hyperons at these K^- beam momenta. We show that the Ξ^- differential and total (absolute and relative) production cross sections at the considered initial momenta reveal a distinct sensitivity to the variations in the scalar Ξ^- nuclear potential at saturation density ρ_0 , studied in the paper, in the low-momentum region of 0.1–0.6 GeV/c. We also demonstrate that for the subthreshold K^- meson momentum of 1.0 GeV/c there is, contrary to the case of its above threshold momentum of 1.3 GeV/c, a strong sensitivity of the transparency ratio for Ξ^- hyperons to the considered changes in the Ξ^- nuclear potential at all outgoing Ξ^- momenta as well, which cannot be masked, as in the case of differential and total observables mentioned above, by that associated with the possible changes in the poorly known experimentally Ξ^-N inelastic cross section. Therefore, the measurement of these absolute and relative observables in a dedicated experiment at the J-PARC Hadron Experimental Facility will provide valuable information on the Ξ^- in-medium properties, which will be complementary to that deduced from the study of the inclusive (K^-, K^+) reactions at incident momenta of 1.6–1.8 GeV/c in the Ξ^- bound and quasi-free regions.

1 Introduction

Essential progress has been made over the last decades in studying the properties of the light K and \bar{K} [1–3], heavy $K^*(892)$ and $\bar{K}^*(892)$ [4–10], $K_1(1270)$ [11–15] mesons as well as of the Λ , Σ , $\Lambda(1405)$, $\Sigma(1385)$, $\Lambda(1520)$ [16–26] hyperons with strangeness $S = -1$ in nuclear matter. The knowledge of these properties is important for understanding both the size and stability of neutron stars, where kaonic and hyperonic matters are expected to appear at their cores, and a partial restoration of chiral symmetry in a dense nuclear medium. What concerns the $S = -2$ sector, the situation, in particular, with the Ξ^-N and Ξ^- -nucleus interactions ¹⁾ is much less conclusive because of the scarcity of the respective Ξ^- scattering, production and hypernuclear data. The experimental knowledge on these interactions is poor currently. The study of Ξ^- hypernuclei and the momentum correlations of p and Ξ^- , produced in relativistic heavy ion collisions, as well as the first principle lattice HAL QCD calculations for masses very close to the physical point provide a valuable information on them at low energies (see, for example, [2, 26, 27, 28]). At present, there are only a few sets of experimental data on the Ξ^- hyperon properties in the nuclear medium. Phenomenological information deduced in Refs. [29, 30] from old emulsion data, from missing-mass measurements [31–34] in the inclusive (K^-, K^+) reaction on nuclear targets at incident momenta of 1.6–1.8 GeV/c in the Ξ^- bound and quasi-free regions with insufficiently good (10 MeV or worse) [31, 32, 33] and moderate (5.4 MeV) [34] energy resolutions, from the analysis the results of these measurements yet in Refs. [35, 36] using Green’s function method of the DWIA as well as the theoretical predictions [37–41] indicate that the Ξ^- cascade hyperon feels only a weak attractive potential in nuclei, the depth of which is not so large, $\sim -(10-20)$ MeV at central nuclear density and at rest ²⁾. Moreover the new recent emulsion KEK-PS E373 [42] and J-PARC E07 [43] experiments, in which the remarkable events named, respectively, ”KISO” and ”IBUKI” were observed, reported the evidence of a likely the Coulomb-assisted nuclear $1p$ single-particle Ξ^- state of the bound Ξ^- - ^{14}N (g.s.) system with binding energy of about 1 MeV, which also testifies in favor of shallow Ξ^- -nucleus potential. The observation of two another hypernuclear events, ”KINKA” and ”IRRAWADDY”, in the E373 and E07 experiments, respectively, gives the first indication of the nuclear $1s$ Ξ^- state of an extremely deep Ξ^- - ^{14}N bound system [44], which also suggests an attractive low-energy potential of the Ξ^- hyperon in nuclear matter. In view of these observations, it is interesting to note that (I) the possibility of the existence of such exotic Ξ hypernuclei as the lightest three-body ΞNN and four-body ΞNNN bound systems has been investigated in Refs. [45] and [46] using, respectively, a Gaussian Expansion Method with two modern ΞN interactions and a pionless halo effective field theory and that (II) the ground state energies of some another exotic Ξ^- hypernuclei – double Ξ^- hypernuclei have been calculated in Ref. [47] within the respective three-body model. To improve essentially our understanding of the Ξ^-N interaction the high-quality data on the doubly strange $S = -2$ hypernuclei are needed. It is expected that in the near future high resolution (up to 1.4 MeV) and high statistics data on the missing-mass spectra for the $^{12}\text{C}(K^-, K^+)$ reaction around the Ξ^- production threshold and the X-ray data on the level shifts and width broadening of the Ξ^- atomic states in the Ξ^- atoms will become available from the planned dedicated E70 and E03 experiments at the J-PARC Hadron Experimental Facility [48].

With regard to the Ξ^- production data and in addition to the aforesaid experimental activities, the Ξ^- yield has been measured at various high beam energies in central Au+Au and Pb+Pb collisions at LHC [49], RHIC [50, 51, 52], SPS [53, 54, 55] and AGS [56]. At SIS energies, the first results on a deep subthreshold production of Ξ^- hyperons in Ar+KCl reactions at beam kinetic energy of 1.76A GeV have been reported by the HADES Collaboration [57]. A surprisingly high Ξ^-

¹⁾The baryon–baryon interactions of the type $\Lambda\Lambda$, $\Lambda\Sigma$ and $\Sigma\Sigma$ are also considered in the strangeness $S = -2$ sector.

²⁾The depth of -14 MeV for the Ξ^- -nucleus potential in the nuclear interior is considered in the literature as the canonical or as the benchmark one [26].

yield over that for Λ hyperons (the abundance ratio) has been observed in this experiment, which exceeds an earlier predictions of a statistical model [58] and a relativistic transport approach [59]. Later on, the Ξ^-/Λ abundance ratio measured by HADES is found to be essentially consistent with the result of calculation within the Relativistic Vlasov-Uehling-Uhlenbeck (RVUU) transport model accounting for the contributions of hyperon–hyperon scattering channels $YY \leftrightarrow \Xi N$ ($Y = \Lambda, \Sigma$), which enhance strongly the yield of Ξ^- [60]. On the other hand, the UrQMD transport model [61], using the YY cross sections provided in [60], could not satisfactorily explain the measured in [57] Ξ^-/Λ ratio. The possible reasons of the discrepancy between the results of Refs. [60] and [61] are discussed in [61]. Also the data on Ξ^- production in $p+p$ and $p+\text{Be}$, $p+\text{Pb}$ collisions have been collected, respectively, in the NA61/SHINE [62] and NA57 [63] experiments performed at the SPS at a beam momentum of 158 GeV/c. Recently, the subthreshold Ξ^- production in collisions of $p(3.5 \text{ GeV})+\text{Nb}$ has been observed for the first time by the HADES Collaboration as well [64]³⁾. It was shown that, in spite of the fact that proton-induced reactions have much simpler dynamics compared to the case of nucleus-nucleus interactions, the available statistical model and two transport approaches (UrQMD and GIBUU) predictions turned out to be substantially lower than the measured in these collisions Ξ^- yield. Contrary to the case of deep subthreshold Ξ^- hyperon production in Ar+KCl reactions at beam kinetic energy of 1.76A GeV [60], the strangeness-exchange reactions $YY \leftrightarrow \Xi N$ are found to be of minor importance for subthreshold Ξ^- creation in pA interactions. This means that a new Ξ^- puzzle appears in these interactions. Possible explanation for it, like in-medium modifications of kaon and Ξ^- hyperon properties, should be studied. It is worth noting that the exclusive photoproduction of Ξ^- and Ξ^0 hyperons in reactions $\gamma p \rightarrow K^+K^+\Xi^-$ and $\gamma p \rightarrow K^+K^+\pi^-\Xi^0$ has been investigated at JLab for near-threshold photon energies using the CLAS detector [65, 66, 67]. Finally, it should be also pointed out that the study of production of ground and excited Ξ baryons is planned to be performed in the future PANDA experiment with an antiproton beam at FAIR [68] and with the upgraded HADES detector in $p+p$ reactions at a beam kinetic energy of 4.5 GeV [69].

In addition to the aforementioned (K^-, K^+) reactions on nuclear targets at beam momenta of 1.6–1.8 GeV/c, the medium modification of the Ξ^- hyperon could be probed directly through the another inclusive near-threshold (K^-, Ξ^-) reactions⁴⁾ on nuclei at J-PARC. The advantage of the latter reactions compared to the former ones is that they have a much cleaner dynamics due to the fact that in them the role played by the two-step processes is expected to be smaller [70]. As a guidance for such future measurements, herein we give the predictions for the absolute differential and total cross sections for near-threshold production of Ξ^- hyperons in $K^-^{12}\text{C} \rightarrow \Xi^- X$ and $K^-^{184}\text{W} \rightarrow \Xi^- X$ reactions at laboratory angles of $\leq 45^\circ$ by incident K^- mesons with momenta of 1.0 and 1.3 GeV/c as well as for their relative yields from these reactions within three different scenarios (see below) for the effective scalar nuclear potential that Ξ^- hyperon feels in the medium. The present calculations are based on a first-collision model, developed in Ref. [71] for the description of the inclusive ϕ meson production on nuclei in near-threshold pion-induced reactions and extended to account for these scenarios for the Ξ^- nuclear potential. Comparison the results of our present calculations with the respective data, which could be taken in future dedicated experiment using K^- beams at the J-PARC Hadron Experimental Facility, will provide a deeper insight into the Ξ^- in-medium properties and information obtained from this comparison will supplement that deduced from the (K^-, K^+) reactions on nuclear targets.

³⁾The kinetic threshold energy for Ξ^- production in free elementary nucleon–nucleon collisions is 3.74 GeV.

⁴⁾Their threshold momentum for free $K^- N$ collisions is about 1.05 GeV/c.

2 Model: direct processes of Ξ^- hyperon production in nuclei

Direct production of Ξ^- hyperons in antikaon–nucleus reactions at near-threshold incident K^- momenta below 1.3 GeV/c can occur in the following K^-p and K^-n elementary processes, which have the lowest free production threshold momentum (≈ 1.05 GeV/c):

$$K^- + p \rightarrow K^+ + \Xi^-, \quad (1)$$

$$K^- + n \rightarrow K^0 + \Xi^-. \quad (2)$$

We can neglect the contribution to the Ξ^- yield from the processes $K^-N \rightarrow K\Xi^-\pi$ with one pion in the final state at initial momenta of interest due to larger their thresholds (≈ 1.34 GeV/c) in free K^-N interactions.

Following [72], for numerical simplicity we will include the in-medium modification of the initial K^- meson as well as of the final K^+ , K^0 mesons and Ξ^- hyperons, involved in the production processes (1), (2), in terms of their average in-medium masses $\langle m_{K^-}^* \rangle$, $\langle m_{K^+}^* \rangle$, $\langle m_{K^0}^* \rangle$ and $\langle m_{\Xi^-}^* \rangle$ instead of their local effective mass $m_{K^-}^*(|\mathbf{r}|)$, $m_{K^+}^*(|\mathbf{r}|)$, $m_{K^0}^*(|\mathbf{r}|)$ and $m_{\Xi^-}^*(|\mathbf{r}|)$ in the in-medium cross sections of these processes, with average in-medium masses defined as:

$$\langle m_h^* \rangle = m_h + U_h \frac{\langle \rho_N \rangle}{\rho_0} + V_{ch}(R_c), \quad (3)$$

where h stands for K^- , K^+ , K^0 and Ξ^- . Here, m_h is the hadron mass in the free space, U_h is the value of its effective scalar nuclear potential (or its in-medium strong interaction mass shift) at normal nuclear matter density ρ_0 , $\langle \rho_N \rangle$ is the average nucleon density and $V_{ch}(R_c)$ is the charged hadron Coulomb potential⁵⁾ of uniform target nucleus charge distribution with a radius of $R_c = 1.22A^{1/3}$ fm taken at the point $|\mathbf{r}| = R_c$ ⁶⁾. In the present work, for nuclei ^{12}C and ^{184}W of interest, the ratio $\langle \rho_N \rangle / \rho_0$, was chosen as 0.55 and 0.76, respectively. For the K^+ mass shift U_{K^+} we will adopt the following momentum-independent option: $U_{K^+} = +22$ MeV [75, 76]. Similar to K^+ ($K^+ = |\bar{s}u \rangle$), the K^0 meson optical potential is expected to be repulsive as well due to its quark content ($K^0 = |\bar{s}d \rangle$) and should be close to that for K^+ in symmetric nuclear matter with equal densities of protons and neutrons [76, 77]. Therefore, the same option will be employed for the K^0 mass shifts U_{K^0} in the case of ^{12}C target nucleus, having $Z = 6$ protons and $N = 6$ neutrons, i.e.: $U_{K^0} = U_{K^+} = +22$ MeV [76, 77, 78]. On the other hand, the K^+ and K^0 mesons are not mass degenerate in an asymmetric nuclear medium [76, 77, 78]. Following Refs. [76, 77], in the subsequent study for the K^0 effective scalar potential depth U_{K^0} we will use the following scenario: $U_{K^0} = +40$ MeV in the case of ^{184}W nucleus, containing $Z = 74$ protons and $N = 110$ neutrons. The K^- nuclear potential at saturation density U_{K^-} , relevant for the incoming K^- meson momentum range of 1.0–1.3 GeV/c, can be chosen as $U_{K^-} = -40$ MeV according to the dispersion analysis performed in Ref. [79].

Let us now determine the Ξ^- hyperon effective scalar potential U_{Ξ^-} , entering into Eq. (3) and appropriate for our present study. In line with the above-mentioned, a nuclear mean-field potential U_{Ξ^-} , acting on a low-momentum Ξ^- hyperon embedded in nuclear matter, is a moderately attractive and could be in the vicinity of -14 MeV at saturation density ρ_0 . Since the accessible range of the Ξ^- hyperon vacuum momenta at incident beam momenta of interest is about of 0.2–0.8 GeV/c (see below), it is helpful to estimate this potential in symmetric nuclear matter also for such in-medium Ξ^- momenta at density ρ_0 . We will rely on the constituent quark model, according to which the quark structure of the Ξ^- hyperon is $\Xi^- = |dss \rangle$. Therefore, the Ξ^- mean-field scalar $U_{S\Xi^-}$ and

⁵⁾This potential for positively and negatively charged hadrons amounts approximately to +3.1 and +15.4 MeV and -3.1 and -15.4 MeV for $^{12}\text{C}_6$ and $^{184}\text{W}_{74}$ nuclei, respectively [73, 74].

⁶⁾Since the incident K^- mesons are absorbed to a large extent on the surface of the nucleus due to their strong initial-state interactions.

vector $U_{V\Xi^-}$ potentials are about 1/3 of those U_{SN} and U_{VN} of a nucleon [80, 81] when in-medium nucleon and Ξ^- hyperon velocities v'_N and v'_{Ξ^-} relative to the nuclear matter are equal to each other, i.e.,

$$U_{S\Xi^-}(v'_{\Xi^-}, \rho_N) = \frac{1}{3}U_{SN}(v'_N, \rho_N),$$

$$U_{V\Xi^-}(v'_{\Xi^-}, \rho_N) = \frac{1}{3}\alpha U_{VN}(v'_N, \rho_N); \quad v'_N = v'_{\Xi^-}. \quad (4)$$

The latter term in Eq. (4) corresponds, to the following relation between the respective in-medium nucleon momentum p'_N and the Ξ^- one p'_{Ξ^-} :

$$p'_N = \frac{\langle m_N^* \rangle}{\langle m_{\Xi^-}^* \rangle} p'_{\Xi^-}. \quad (5)$$

However, for reasons of numerical simplicity, calculating the Ξ^- -nucleus single-particle potential (or the so-called Schrödinger equivalent potential $V_{\Xi^-A}^{\text{SEP}}$), we will employ in expression (5) free space nucleon and Ξ^- hyperon masses m_N and m_{Ξ^-} instead of their average in-medium masses $\langle m_N^* \rangle$ and $\langle m_{\Xi^-}^* \rangle$. Then, this potential $V_{\Xi^-A}^{\text{SEP}}$ can be defined as [80, 81]⁷⁾:

$$V_{\Xi^-A}^{\text{SEP}}(p'_{\Xi^-}, \rho_N) = \sqrt{[m_{\Xi^-} + U_{S\Xi^-}(p'_{\Xi^-}, \rho_N)]^2 + (p'_{\Xi^-})^2} + U_{V\Xi^-}(p'_{\Xi^-}, \rho_N) - \sqrt{m_{\Xi^-}^2 + (p'_{\Xi^-})^2}. \quad (6)$$

The relation between the potentials U_{Ξ^-} and $V_{\Xi^-A}^{\text{SEP}}$ at normal nuclear matter density is given by

$$U_{\Xi^-}(p'_{\Xi^-}) = \frac{\sqrt{m_{\Xi^-}^2 + (p'_{\Xi^-})^2}}{m_{\Xi^-}} V_{\Xi^-A}^{\text{SEP}}(p'_{\Xi^-}). \quad (7)$$

Employing the momentum-dependent parametrization for the nucleon scalar and vector potentials at saturation density ρ_0 from [82]

$$U_{SN}(p'_N, \rho_0) = -\frac{494.2272}{1 + 0.3426\sqrt{p'_N/p_F}} \text{ MeV}, \quad (8)$$

$$U_{VN}(p'_N, \rho_0) = \frac{420.5226}{1 + 0.4585\sqrt{p'_N/p_F}} \text{ MeV} \quad (9)$$

(where $p_F = 1.35 \text{ fm}^{-1} = 0.2673 \text{ GeV}/c$) and using Eqs. (4)–(6), we calculated the momentum dependence of potential $V_{\Xi^-A}^{\text{SEP}}$ at density ρ_0 . In doing so, we have also made an adjustment by multiplying the vector nucleon potential in Eq. (4) by a factor α of $\alpha = 1.068$ [78] to get for Λ hyperon potential $V_{\Lambda A}^{\text{SEP}}$ at zero momentum and at density ρ_0 a value consistent with the experimental one of $-(32 \pm 2)$ MeV, extracted from data on binding energies of Λ single-particle states in nuclei [83]. The adjusted in such manner Ξ^- potential $V_{\Xi^-A}^{\text{SEP}}$ is shown in figure 1 by solid curve. One can see that in this case the Ξ^- -nucleus potential is attractive for all momenta $\leq 0.8 \text{ GeV}/c$ with the value of $V_{\Xi^-A}^{\text{SEP}}(0) = U_{\Xi^-}(0) \approx -15 \text{ MeV}$, whereas it will be repulsive for higher momenta. The above value is well consistent with the Ξ^- -nucleus Woods-Saxon potential depths of about -16 and -14 MeV, deduced from the analysis of the data in the Ξ^- -bound state region of the missing-mass spectra for $^{12}\text{C}(K^-, K^+)$ reaction taken by the KEK-PS E224 [31] and BNL-AGS E885 [32] Collaborations at incident momenta of 1.6 and 1.8 GeV/c, respectively. Moreover, it is also in good agreement with that of $\approx -16 \text{ MeV}$ for the Ξ^- in-medium mass shift predicted very recently in Ref. [84] within the framework of the in-medium modified chiral soliton model. In addition, results for two Ξ^- single-particle potentials for symmetric nuclear matter from the recent literature are shown in Fig.

⁷⁾The space-like component of the Ξ^- vector self-energy is ignored here.

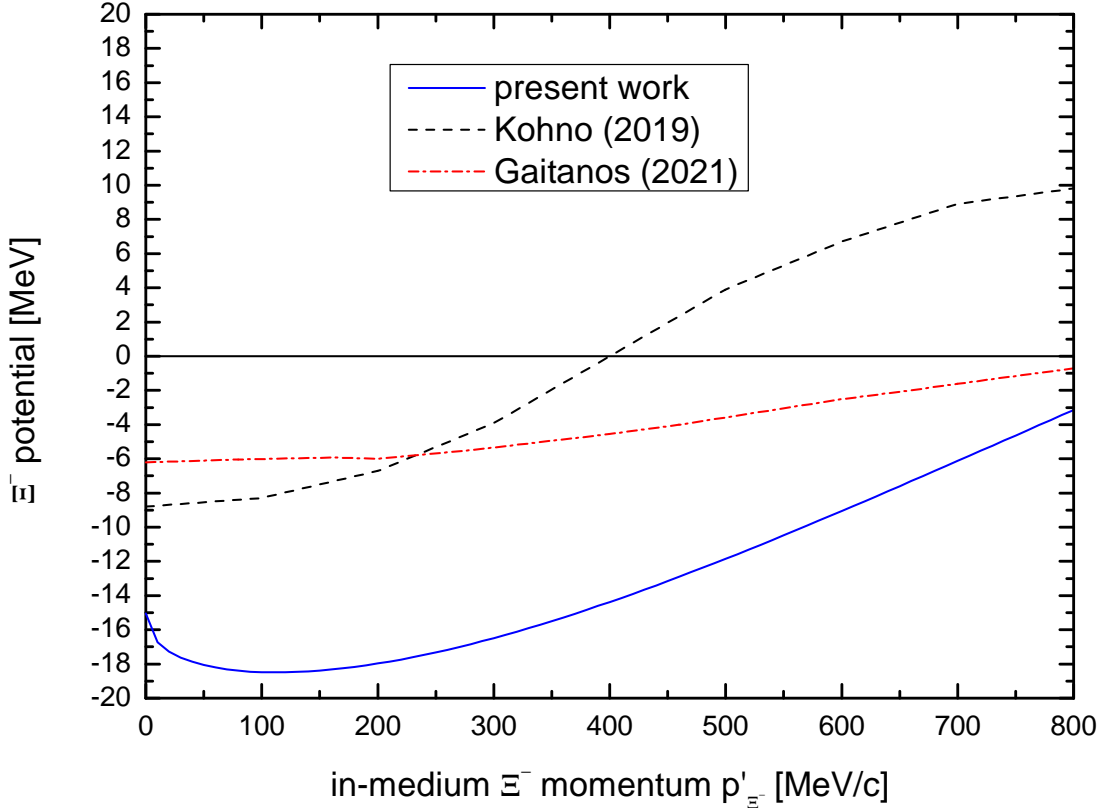


Figure 1: (Color online) Momentum dependence of the Schrödinger equivalent Ξ^- hyperon potential at density ρ_0 . For notation see the text.

1 as well, namely: the chiral effective field theory (EFT) at the next-to-leading order (NLO) based potential [74] (dashed curve) and the NLD potential [85] (dotted-dashed curve). It is seen that the latter potential is more weakly attractive at all momenta considered than that, calculated in the present work. Its momentum dependence is a relatively weak with the value of about -6 MeV at zero momentum with respect to the surrounding nuclear matter. It is worth noting that this potential is compatible [85] with recently updated lattice QCD calculations [86] (cf. [87]), which show a slightly more shallow Ξ^- single-particle potential in the nuclear medium at the density ρ_0 for momenta below ≈ 600 MeV/c with the central value of -4 MeV with the statistical error about ± 2 MeV at zero momentum and rather moderate repulsive potential at higher momenta. It should be pointed out that this lattice QCD based potential at zero momentum relative to the bulk matter is consistent with the corresponding values of -3.8 to -5.5 MeV predicted in Ref. [88] within the updated chiral EFT at the NLO (cf. [89]). An essential difference between present, NLD potentials and that from Ref. [74] is that the latter shows a much stronger momentum dependence and turns from attractive with the value of $V_{\Xi^-A}^{\text{SEP}}(0) \approx -9$ MeV, which is also in line with that of -7 MeV predicted in Ref. [90] for the Nijmegen ESC08c potential, to repulsive at about 400 MeV/c momentum and reaches the value $\approx +10$ MeV at Ξ^- momentum of about 800 MeV/c. On the other hand, contrary to the above, the in-medium calculations [91] and [92], based on the baryon-baryon interactions in the $S = -2$ sector derived using the chiral EFT in the leading order (LO), yield $V_{\Xi^-A}^{\text{SEP}}(0) \approx +6$ MeV [91] and $\approx +9$ MeV [88, 92] at normal nuclear density. So, nowadays there are

considerable uncertainties in determining the Ξ^- nuclear potential both at threshold and at finite momenta below 1 GeV/c. These uncertainties could be essentially reduced, comparing, for example, the results of the present model calculations with the respective precise experimental data on direct Ξ^- production on nuclei. These data could be obtained in future dedicated experiment at J-PARC using near-thresholds K^- beams. Here, the Ξ^- hyperons could be registered via the hadronic decay chain $\Xi^- \rightarrow \Lambda\pi^- \rightarrow p\pi^-\pi^-$, which has a total branching ratio of about 64%. It should be noted that a similar comparison of a model cross sections with data on η' meson photoproduction off carbon and niobium target nuclei was adopted in Refs. [93, 94] to extract its effective scalar potential in the nuclear medium. It should be noted that some hint on the possible strength of the Ξ^- optical potential for Ξ^- - ^8Li system at momenta of interest comes from the recent analysis [95] of the BNL-E906 measurement of the spectrum of the $^9\text{Be}(K^-, K^+)$ reaction at incident K^- momentum of 1.8 GeV/c and K^+ forward-direction lab angles of $\theta_{K^+} = 1.5^\circ - 8.5^\circ$ in the Ξ^- quasi-free region within the DWIA using the optimal Fermi-averaged $K^-p \rightarrow K^+\Xi^-$ amplitude. The strength of (-17 ± 6) MeV for this potential in the Woods-Saxon prescription was deduced from this analysis in the momentum transfer region $q \simeq 390 - 600$ MeV/c [95]. If we assume that $p'_{\Xi^-} = q$, then this value can be to some extent interpreted as Ξ^- -nucleus potential well depth in the momentum range of $\simeq 390 - 600$ MeV/c and, therefore, can be compared with the predictions presented in Fig. 1. It can be seen that only our calculation, which gives $V_{\Xi^-A}^{\text{SEP}}(390 \text{ MeV/c}) \approx -14$ MeV and $V_{\Xi^-A}^{\text{SEP}}(600 \text{ MeV/c}) \approx -9$ MeV, is compatible with the result of [95] over the given momentum range. Accounting for the relation (7) between the potentials U_{Ξ^-} and $V_{\Xi^-A}^{\text{SEP}}$ at normal nuclear matter density and using our results shown in Fig. 1, we can readily get that the former one varies from ≈ -18 MeV to -10 MeV when Ξ^- momentum changes from ~ 200 MeV/c to 600 MeV/c with average value of ≈ -14 MeV, which is quite consistent with that inferred by Khaustov *et al.* [32] at zero momentum. Therefore, it is natural to employ for the quantity U_{Ξ^-} in our work the canonical value of $U_{\Xi^-} = -14$ MeV in whole Ξ^- momentum range studied (see, also [96, 97, 98]). On the other hand, in this momentum range this potential, as follows from Fig. 1 and Eq. (7), might be repulsive at Ξ^- hyperon momenta > 600 MeV/c reaching the value $\sim +14$ MeV at momentum ~ 1.0 GeV/c. Therefore, to account for all the possible variations in the Ξ^- nuclear potential at all outgoing Ξ^- momenta, we will also both ignore it ⁸⁾ in our calculations and use for it in them the value of $+14$ MeV. Thus, the results will be presented with the three basic cases of a Ξ^- potential: i) $U_{\Xi^-} = -14$ MeV, ii) $U_{\Xi^-} = 0$ MeV and iii) $U_{\Xi^-} = +14$ MeV (cf. [74]) at finite momenta, accessible in calculation of the Ξ^- production in K^-A reactions at beam momenta of interest for both target nuclei of ^{12}C and ^{184}W ⁹⁾. In addition, to extend the range of applicability of our model and to see the sensitivity of

⁸⁾Which corresponds to almost zero Ξ^- potential at finite momenta of interest, predicted in particular in Ref. [86].

⁹⁾It should be noticed that this assumes a purely isoscalar Ξ^- potential $U_{\Xi^-}^{\text{isoscalar}}(r)$, associated with the total nuclear density $\rho_n(r) + \rho_p(r)$, for both these targets and does not account for the contribution to the total strong interaction Ξ^- potential $U_{\Xi^-}(r)$ from the isovector one $U_{\Xi^-}^{\text{isovector}}(r)$, appearing in the neutron-rich nuclei due to the neutron excess density $\rho_n(r) - \rho_p(r)$. The latter might be nonnegligible in the ^{184}W nucleus. Let us estimate it. According to [2], these low-energy potentials can be expressed as: $U_{\Xi^-}^{\text{isoscalar}}(r) = \alpha_0[\rho_n(r) + \rho_p(r)]$ and $U_{\Xi^-}^{\text{isovector}}(r) = \alpha_1[\rho_n(r) - \rho_p(r)]$. Assuming that $\rho_{n(p)}(r) = N(Z)\rho(r)$, we get that the ratio $U_{\Xi^-}^{\text{isovector}}(r)/U_{\Xi^-}^{\text{isoscalar}}(r)$ is equal to $[(N - Z)/A][\alpha_1/\alpha_0]$. The ratio α_1/α_0 can be evaluated as follows. Take for example the values $U_{\Xi^-}(0) = U_{\Xi^-}^{\text{isoscalar}}(0) = 2\alpha_0\rho_n(0) = -4$ MeV in symmetric nuclear matter and $U_{\Xi^-}(0) = 2\alpha_0\rho_n(0) + 2\alpha_1\rho_n(0) = +6$ MeV in pure neutron matter of the recent HAL-QCD calculation [86]. Then we easily obtain that $\alpha_1/\alpha_0 = +10 \text{ MeV} / -4 \text{ MeV} = -2.5$. As a result, the ratio $U_{\Xi^-}^{\text{isovector}}(r)/U_{\Xi^-}^{\text{isoscalar}}(r)$ for $[(N - Z)/A] = 0.2$ (^{184}W) is -0.5 , which is nonnegligible. But if we take the value of -24.3 MeV for the isoscalar Ξ^- hyperon potential, suggested by the very recent analysis of Ref. [99] of the Ξ^- capture events in light nuclear emulsion identified in KEK and J-PARC experiments [42, 43], and retain the same value of $+6$ MeV as above for its potential in pure neutron matter, we get for the ratio $U_{\Xi^-}^{\text{isovector}}(r)/U_{\Xi^-}^{\text{isoscalar}}(r)$ for $[(N - Z)/A] = 0.2$ a substantially smaller value of -0.25 . The aforementioned means that a more realistic analysis of the Ξ^- hyperon production in heavy asymmetric targets should account for in principle not only the isoscalar Ξ^- -nucleus potential, but also and an isovector one. However, since the main difference between the Ξ^- nuclear potentials in light (symmetric) and heavy (asymmetric) nuclei is coming from the Coulomb forces, which are included

the Ξ^- production cross sections from the direct processes (1), (2) to the potential U_{Ξ^-} , we will yet adopt in some calculations three another additional representative options for this potential, namely: i) $U_{\Xi^-} = -25$ MeV, ii) $U_{\Xi^-} = -15$ MeV and iii) $U_{\Xi^-} = -5$ MeV, covering in view of the above-mentioned the bulk of the low-energy theoretical and experimental information presently available in this field.

The total energy E'_h of the hadron inside the nuclear matter is expressed via its average effective mass $\langle m_h^* \rangle$ defined above and its in-medium momentum \mathbf{p}'_h by the expression [72]:

$$E'_h = \sqrt{(\mathbf{p}'_h)^2 + (\langle m_h^* \rangle)^2}. \quad (10)$$

The momentum \mathbf{p}'_h is related to the vacuum hadron momentum \mathbf{p}_h as follows [72]:

$$E'_h = \sqrt{(\mathbf{p}'_h)^2 + (\langle m_h^* \rangle)^2} = \sqrt{\mathbf{p}_h^2 + m_h^2} = E_h, \quad (11)$$

where E_h is the hadron total energy in vacuum. It is of further interest to calculate, using the

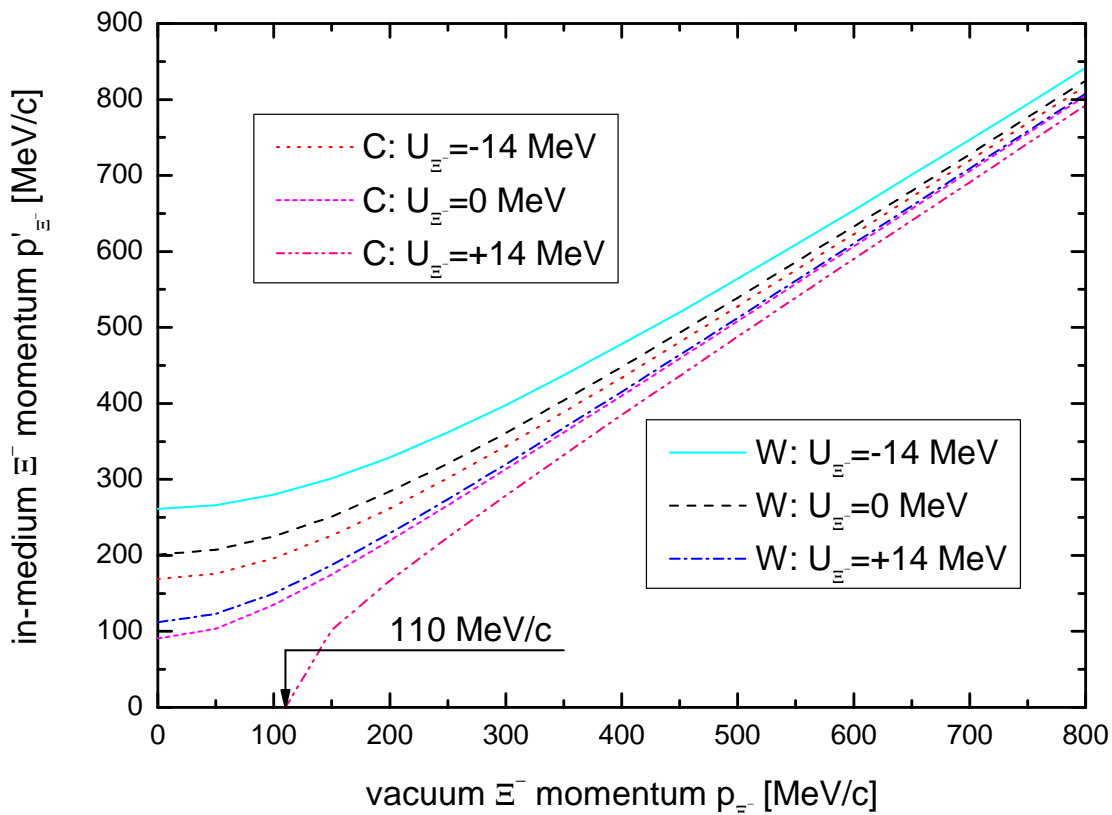


Figure 2: (Color online) Vacuum Ξ^- hyperon momentum dependence of its in-medium momentum for ^{12}C and ^{184}W nuclei at various values of the strong interaction mass shift U_{Ξ^-} indicated in the inset.

relations (3) and (11), the vacuum Ξ^- hyperon momentum dependence of its in-medium momentum

in our model, one may hope that the role played by the real isovector Ξ^- optical potential in this production will be moderate. Its rigorous evaluation is beyond the scope of the present work.

for ^{12}C and ^{184}W target nuclei for the adopted three options for the effective scalar potential U_{Ξ^-} . The results of such calculations are shown in Fig. 2. We have that $p'_{\Xi^-}(U_{\Xi^-} = -14 \text{ MeV}) > p'_{\Xi^-}(U_{\Xi^-} = 0 \text{ MeV}) > p_{\Xi^-}$ for tungsten nucleus. In the case of carbon nucleus we also have that $p'_{\Xi^-}(U_{\Xi^-} = -14 \text{ MeV}) > p'_{\Xi^-}(U_{\Xi^-} = 0 \text{ MeV}) > p_{\Xi^-}$, but contrary to the W nucleus case $p'_{\Xi^-}(U_{\Xi^-} = +14 \text{ MeV}) < p_{\Xi^-}$. The effect of the cascade particle potential U_{Ξ^-} on in-medium renormalisation of its vacuum momentum is significant at the vacuum Ξ^- momenta less than 600 MeV/c. Whereas, at higher Ξ^- momenta its impact on this renormalisation is not substantial. Thus, for example, the differences $p'_{\Xi^-}(U_{\Xi^-} = -14 \text{ MeV}) - p'_{\Xi^-}(U_{\Xi^-} = 0 \text{ MeV})$, $p'_{\Xi^-}(U_{\Xi^-} = 0 \text{ MeV}) - p'_{\Xi^-}(U_{\Xi^-} = +14 \text{ MeV})$ are $\sim 20\%$ and 3% for momenta p_{Ξ^-} of 200 and 600 MeV/c, respectively, for both considered nuclei. This will lead, in particular, to different sensitivity of the Ξ^- hyperon momentum distributions to the potential U_{Ξ^-} , which it feels inside the nuclear matter, at low and high Ξ^- momenta (see Figs. 5 and 6 given below).

The Ξ^- -nucleon elastic cross section is expected to be $\sim 5\text{--}15 \text{ mb}$ in the studied Ξ^- momentum range of 0.2–1.0 GeV/c [88, 89, 92, 100, 101, 102] of our main interest. The Ξ^- mean "free" path up to quasielastic rescattering can be evaluated as $\lambda_{\Xi^-}^{\text{el}} = 1/(\langle \rho_N \rangle \sigma_{\Xi^-N}^{\text{el}})$, where $\sigma_{\Xi^-N}^{\text{el}}$ is the appropriate Ξ^-N elastic cross section. Using $\langle \rho_N \rangle = 0.55\rho_0$ (^{12}C) and $\langle \rho_N \rangle = 0.76\rho_0$ (^{184}W), $\rho_0 = 0.16 \text{ fm}^{-3}$ and as an estimate of $\sigma_{\Xi^-N}^{\text{el}}$ for Ξ^- momenta of interest the value of 10 mb, we obtain that $\lambda_{\Xi^-}^{\text{el}} \approx 11 \text{ fm}$ for ^{12}C and $\lambda_{\Xi^-}^{\text{el}} \approx 8 \text{ fm}$ for ^{184}W . These values are larger, respectively, than the radii of ^{12}C and ^{184}W , which are approximately 3 and 7.4 fm. Therefore, we will neglect quasielastic Ξ^-N rescatterings in the present study and will do not consider the loss and gain of the Ξ^- flux in the nucleus inside the wide laboratory solid Ξ^- production angle under consideration. Then, accounting for that the in-medium threshold energies $\sqrt{s_{\text{th}}^*} = \langle m_{K^+}^* \rangle + \langle m_{\Xi^-}^* \rangle$ and $\sqrt{s_{\text{th}}^*} = \langle m_{K^0}^* \rangle + \langle m_{\Xi^-}^* \rangle$ of the processes (1) and (2) are practically equal to each other for both considered target nuclei and the fact that the total cross sections of these processes are described by the same functional form [60] as well as taking into account the attenuation of the incident antikaon and the final Ξ^- hyperon in the nuclear matter in terms, respectively, of the K^-N total cross section $\sigma_{K^-N}^{\text{tot}}$ and the total inelastic Ξ^-N cross section $\sigma_{\Xi^-N}^{\text{in}}$, we represent, according to Ref. [71], the inclusive differential cross section for the production of Ξ^- hyperons with vacuum momentum \mathbf{p}_{Ξ^-} on nuclei in the direct processes (1), (2) as follows:

$$\frac{d\sigma_{K^-A \rightarrow \Xi^-X}^{\text{(dir)}}(\mathbf{p}_{K^-}, \mathbf{p}_{\Xi^-})}{d\mathbf{p}_{\Xi^-}} = I_V[A, \theta_{\Xi^-}] \left\langle \frac{d\sigma_{K^-p \rightarrow K^+\Xi^-}(\mathbf{p}'_{K^-}, \mathbf{p}'_{\Xi^-})}{d\mathbf{p}'_{\Xi^-}} \right\rangle_A \frac{d\mathbf{p}'_{\Xi^-}}{d\mathbf{p}_{\Xi^-}}, \quad (12)$$

where

$$I_V[A, \theta_{\Xi^-}] = A \int_0^R r_{\perp} dr_{\perp} \int_{-\sqrt{R^2-r_{\perp}^2}}^{\sqrt{R^2-r_{\perp}^2}} dz \rho(\sqrt{r_{\perp}^2+z^2}) \exp \left[-\sigma_{K^-N}^{\text{tot}}(p_{K^-}) A \int_{-\sqrt{R^2-r_{\perp}^2}}^z \rho(\sqrt{r_{\perp}^2+x^2}) dx \right] \quad (13)$$

$$\times \int_0^{2\pi} d\varphi \exp \left[-\sigma_{\Xi^-N}^{\text{in}}(p'_{\Xi^-}) A \int_0^{l(\theta_{\Xi^-}, \varphi)} \rho(\sqrt{x^2+2a(\theta_{\Xi^-}, \varphi)x+b+R^2}) dx \right];$$

$$a(\theta_{\Xi^-}, \varphi) = z \cos \theta_{\Xi^-} + r_{\perp} \sin \theta_{\Xi^-} \cos \varphi, \quad b = r_{\perp}^2 + z^2 - R^2, \quad (14)$$

$$l(\theta_{\Xi^-}, \varphi) = \sqrt{a^2(\theta_{\Xi^-}, \varphi) - b - a(\theta_{\Xi^-}, \varphi)}, \quad (15)$$

$$\sigma_{K^-N}^{\text{tot}}(p_{K^-}) = \frac{Z}{A} \sigma_{K^-p}^{\text{tot}}(p_{K^-}) + \frac{N}{A} \sigma_{K^-n}^{\text{tot}}(p_{K^-}), \quad (16)$$

$$\sigma_{\Xi^-N}^{\text{in}}(p'_{\Xi^-}) = \frac{Z}{A} \sigma_{\Xi^-p}^{\text{in}}(p'_{\Xi^-}) + \frac{N}{A} \sigma_{\Xi^-n}^{\text{in}}(p'_{\Xi^-}) \quad (17)$$

and

$$\left\langle \frac{d\sigma_{K^-p \rightarrow K^+\Xi^-}(\mathbf{p}'_{K^-}, \mathbf{p}'_{\Xi^-})}{d\mathbf{p}'_{\Xi^-}} \right\rangle_A = \int \int P_A(\mathbf{p}_t, E) d\mathbf{p}_t dE \quad (18)$$

$$\times \left\{ \frac{d\sigma_{K^-p \rightarrow K^+\Xi^-}[\sqrt{s^*}, \langle m_{K^+}^* \rangle, \langle m_{\Xi^-}^* \rangle, \mathbf{p}'_{\Xi^-}]}{d\mathbf{p}'_{\Xi^-}} \right\}, \quad (19)$$

$$s^* = (E'_{K^-} + E_t)^2 - (\mathbf{p}'_{K^-} + \mathbf{p}_t)^2, \quad (19)$$

$$E_t = M_A - \sqrt{(-\mathbf{p}_t)^2 + (M_A - m_N + E)^2}. \quad (20)$$

Here, $d\sigma_{K^-p \rightarrow K^+\Xi^-}[\sqrt{s^*}, \langle m_{K^+}^* \rangle, \langle m_{\Xi^-}^* \rangle, \mathbf{p}'_{\Xi^-}]/d\mathbf{p}'_{\Xi^-}$ is the off-shell inclusive differential cross section for the production of K^+ meson and Ξ^- hyperon with modified masses $\langle m_{K^+}^* \rangle$ and $\langle m_{\Xi^-}^* \rangle$, respectively. The Ξ^- hyperon is produced with in-medium momentum \mathbf{p}'_{Ξ^-} in process (1) at the K^-p center-of-mass energy $\sqrt{s^*}$. E'_{K^-} and \mathbf{p}'_{K^-} are in-medium total energy and momentum of the incident antikaon, which are related by the equation (10); $\rho(\mathbf{r})$ and $P_A(\mathbf{p}_t, E)$ are the local nucleon density and the spectral function of the target nucleus A normalized to unity (the detailed information about these quantities, used in our calculations, is given in Refs. [71, 75, 103, 104]); \mathbf{p}_t and E are the internal momentum and removal energy of the target proton involved in the collision process (1); Z and N are the numbers of protons and neutrons in the target nucleus ($A = Z + N$), M_A and R are its mass and radius; m_N is the free space nucleon mass; θ_{Ξ^-} is the polar angle of vacuum momentum \mathbf{p}_{Ξ^-} in the laboratory system with z-axis directed along the vacuum momentum \mathbf{p}_{K^-} of the incident antikaon beam; $\sigma_{K^-p}^{\text{tot}}(p_{K^-})$ and $\sigma_{K^-n}^{\text{tot}}(p_{K^-})$ are the total cross section of the free [105, 106] K^-p and K^-n interactions¹⁰⁾ at vacuum beam momenta of 1.0 and 1.3 GeV/c¹¹⁾. At these momenta, $\sigma_{K^-p}^{\text{tot}} \approx 50$ and 30 mb. And $\sigma_{K^-n}^{\text{tot}} \approx 40$ and 30 mb [107]. With these, the quantity $\sigma_{K^-N}^{\text{tot}}$, entering into Eqs. (13) and (16), amounts approximately to 45 and 30 mb for initial momenta of 1.0 and 1.3 GeV/c for both considered target nuclei $^{12}\text{C}_6$ and $^{184}\text{W}_{74}$. We will employ these values in our calculations. In Eq. (12) it is assumed that the Ξ^- hyperon production cross sections in K^-p and K^-n interactions (1) and (2) are the same [60]. In addition, it is suggested that the ways of the incident antikaon from the vacuum to the production point inside the nucleus and of the produced cascade hyperon at this point out of the nucleus are not disturbed by the weak K^- and Ξ^- nuclear potentials, considered in the present work, by the respective attractive Coulomb potentials as well as by rare K^-N and Ξ^-N elastic rescatterings. As a result, the in-medium antikaon and hyperon momenta \mathbf{p}'_{K^-} and \mathbf{p}'_{Ξ^-} are assumed to be parallel, respectively, to the vacuum ones \mathbf{p}_{K^-} and \mathbf{p}_{Ξ^-} and the relation between them is given by Eq. (11).

In line with [71, 72], we suppose that the off-shell differential cross section $d\sigma_{K^-p \rightarrow K^+\Xi^-}[\sqrt{s^*}, \langle m_{K^+}^* \rangle, \langle m_{\Xi^-}^* \rangle, \mathbf{p}'_{\Xi^-}]/d\mathbf{p}'_{\Xi^-}$ for Ξ^- production in process (1) is equivalent to the respective on-shell cross section calculated for the off-shell kinematics of this process as well as for the final K^+ meson and Ξ^- hyperon in-medium masses $\langle m_{K^+}^* \rangle$ and $\langle m_{\Xi^-}^* \rangle$, respectively. Accounting for the results given in Ref. [71] and assuming that the Ξ^- angular distribution in reaction (1) is isotropic in the K^-p c.m.s. at beam momenta of interest (cf. [98, 108]¹²⁾), we obtain the following

¹⁰⁾ It should be mentioned that the use of the total K^-p and K^-n cross sections instead of the inelastic ones in Eqs. (13), (16) is caused by the fact that the K^- energy loss in nucleus, associated with the K^- meson quasielastic rescatterings on the intranuclear nucleons, will lead to a substantial reduction of its possibility to create a Ξ^- hyperon in the processes (1) and (2) at considered near-threshold laboratory incident antikaon momenta, or in other words, will cause the additional to the genuine "absorption" of the K^- meson flux in nuclear matter with respect to the Ξ^- creation in these processes.

¹¹⁾ We assume that $\sigma_{K^-p}^{\text{tot}}(p'_{K^-}) \approx \sigma_{K^-p}^{\text{tot}}(p_{K^-})$ and $\sigma_{K^-n}^{\text{tot}}(p'_{K^-}) \approx \sigma_{K^-n}^{\text{tot}}(p_{K^-})$. This is well justified due to the following. For example, for incident K^- meson momentum of $p_{K^-} = 1.0$ GeV/c its in-medium momentum p'_{K^-} is equal to 1.012 and 1.021 GeV/c for ^{12}C and ^{184}W , respectively. And according to [107], we have that $\sigma_{K^-p(K^-n)}^{\text{tot}}(p'_{K^-} = 1.012, 1.021 \text{ GeV/c}) \approx \sigma_{K^-p(K^-n)}^{\text{tot}}(p_{K^-} = 1.0 \text{ GeV/c})$.

¹²⁾ Presented here experimental angular distribution of the reaction $K^-p \rightarrow K^+\Xi^-$ shows practically an isotropic behavior at the lowest c.m.s. collision energy of 1.95 GeV (or at the lowest K^- beam momentum of 1.34 GeV/c).

expression for this differential cross section:

$$\begin{aligned} \frac{d\sigma_{K^-p \rightarrow K^+\Xi^-}[\sqrt{s^*}, \langle m_{K^+}^* \rangle, \langle m_{\Xi^-}^* \rangle, \mathbf{p}'_{\Xi^-}]}{d\mathbf{p}'_{\Xi^-}} &= \frac{\pi}{I_2[s^*, \langle m_{K^+}^* \rangle, \langle m_{\Xi^-}^* \rangle] E'_{\Xi^-}} \quad (21) \\ &\times \frac{\sigma_{K^-p \rightarrow K^+\Xi^-}(\sqrt{s^*}, \sqrt{s_{\text{th}}^*})}{4\pi} \\ &\times \frac{1}{(\omega + E_t)} \delta \left[\omega + E_t - \sqrt{(\langle m_{K^+}^* \rangle)^2 + (\mathbf{Q} + \mathbf{p}_t)^2} \right], \end{aligned}$$

where

$$I_2[s^*, \langle m_{K^+}^* \rangle, \langle m_{\Xi^-}^* \rangle] = \frac{\pi}{2} \frac{\lambda[s^*, (\langle m_{K^+}^* \rangle)^2, (\langle m_{\Xi^-}^* \rangle)^2]}{s^*}, \quad (22)$$

$$\lambda(x, y, z) = \sqrt{[x - (\sqrt{y} + \sqrt{z})^2][x - (\sqrt{y} - \sqrt{z})^2]}, \quad (23)$$

$$\omega = E'_{K^-} - E'_{\Xi^-}, \quad \mathbf{Q} = \mathbf{p}'_{K^-} - \mathbf{p}'_{\Xi^-}. \quad (24)$$

Here, $\sigma_{K^-p \rightarrow K^+\Xi^-}(\sqrt{s^*}, \sqrt{s_{\text{th}}^*})$ is the "in-medium" total cross section of reaction (1) having the threshold energy $\sqrt{s_{\text{th}}^*}$ defined above. In line with the above-mentioned, it is equivalent to the vacuum cross section $\sigma_{K^-p \rightarrow K^+\Xi^-}(\sqrt{s}, \sqrt{s_{\text{th}}})$, in which the vacuum threshold energy $\sqrt{s_{\text{th}}} = m_{K^+} + m_{\Xi^-} = 1.8154$ GeV is replaced by the in-medium one $\sqrt{s_{\text{th}}^*}$ and the free center-of-mass energy squared s , presented by the formula

$$s = (E_{K^-} + m_N)^2 - \mathbf{p}_{K^-}^2, \quad (25)$$

is replaced by the in-medium one s^* , defined by the expression (19).

For the free total cross section $\sigma_{K^-p \rightarrow K^+\Xi^-}(\sqrt{s}, \sqrt{s_{\text{th}}})$ we have adopted the following parametrization, suggested in Ref. [60]:

$$\sigma_{K^-p \rightarrow K^+\Xi^-}(\sqrt{s}, \sqrt{s_{\text{th}}}) = 235.6 \left(1 - \sqrt{s_{\text{th}}}/\sqrt{s}\right)^{2.4} \left(\sqrt{s_{\text{th}}}/\sqrt{s}\right)^{16.6} \text{ [mb]}. \quad (26)$$

As is seen from Fig. 3, it (solid curve) fits well the data (full squares), taken from the compilation of Flaminio *et al.* [107]. As can also be seen from this figure, the on-shell cross section $\sigma_{K^-p \rightarrow K^+\Xi^-}$ amounts approximately to 100 μb for the initial antikaon momentum of 1.3 GeV/c, corresponding to the excess energy $\sqrt{s} - \sqrt{s_{\text{th}}} = 117$ MeV. This offers the possibility of measuring the Ξ^- yield in near-threshold K^-A reactions at the J-PARC Hadron Experimental Facility with sizable strength using high-intensity separated secondary antikaon beams in the K1.8 and K1.8BR beamlines [48].

Accounting for the fact that in the considered initial momentum region Ξ^- hyperons are mainly emitted, due to the kinematics, in a narrow cone along the beam line ¹³⁾, we will calculate the Ξ^- momentum differential and total production cross sections on ^{12}C and ^{184}W targets for the laboratory solid angle $\Delta\Omega_{\Xi^-} = 0^\circ \leq \theta_{\Xi^-} \leq 45^\circ$, and $0 \leq \varphi_{\Xi^-} \leq 2\pi$. Here, φ_{Ξ^-} is the azimuthal angle of the Ξ^- momentum \mathbf{p}_{Ξ^-} in the laboratory system. Then, integrating the full inclusive differential cross section (12) over this angular domain with taking into account that in Eqs. (12)–(15) we suppose that the direction of the Ξ^- hyperon momentum is not changed during its propagation inside the nucleus from the production point in it to the vacuum, we can represent the differential cross section for Ξ^- hyperon production in antikaon-induced reactions from the direct processes (1), (2), corresponding to this angle, in the following form:

$$\frac{d\sigma_{K^-A \rightarrow \Xi^- X}^{(\text{dir})}(p_{K^-}, p_{\Xi^-})}{dp_{\Xi^-}} = \int_{\Delta\Omega_{\Xi^-}} d\Omega_{\Xi^-} \frac{d\sigma_{K^-A \rightarrow \Xi^- X}^{(\text{dir})}(\mathbf{p}_{K^-}, \mathbf{p}_{\Xi^-})}{d\mathbf{p}_{\Xi^-}} p_{\Xi^-}^2 \quad (27)$$

¹³⁾ Thus, for instance, at a beam momentum of 1.3 GeV/c the Ξ^- laboratory production polar angles in reaction (1) proceeding on the target proton being at rest are $\leq 19.65^\circ$.

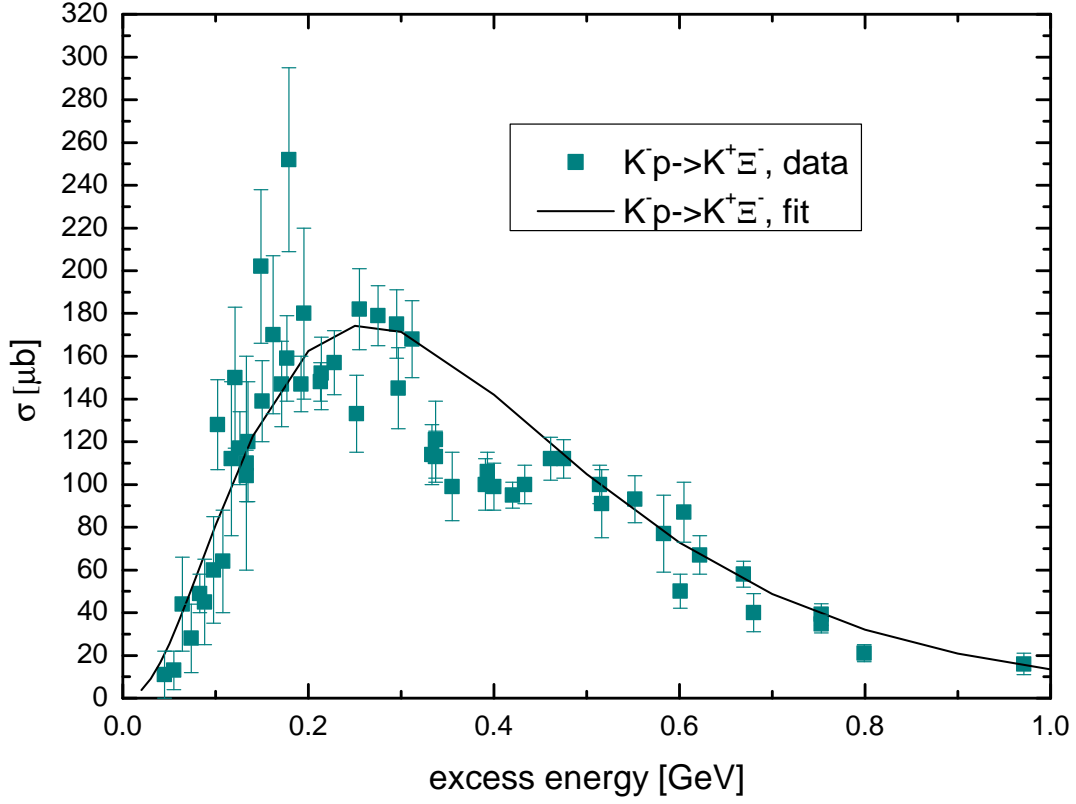


Figure 3: (Color online) Total cross section for the reaction $K^-p \rightarrow K^+\Xi^-$ as function of the available excess energy $\sqrt{s} - \sqrt{s_{\text{th}}}$ above the threshold $\sqrt{s_{\text{th}}}$. For notation see the text.

$$= 2\pi \left(\frac{p_{\Xi^-}}{p'_{\Xi^-}} \right)_{\cos 45^\circ} \int_0^1 d \cos \theta_{\Xi^-} I_V[A, \theta_{\Xi^-}] \left\langle \frac{d\sigma_{K^-p \rightarrow K^+\Xi^-}(p'_{K^-}, p'_{\Xi^-}, \theta_{\Xi^-})}{dp'_{\Xi^-} d\Omega_{\Xi^-}} \right\rangle_A.$$

We will consider also the effects from Ξ^- in-medium modification and from Ξ^- absorption in nuclear matter on the momentum dependence of the following relative observable – the transparency ratio T_A defined as the ratio between the inclusive differential cascade production cross section (27) on a heavy nucleus and a light one (^{12}C):

$$T_A(p_{K^-}, p_{\Xi^-}) = \frac{12 d\sigma_{K^-A \rightarrow \Xi^-X}^{(\text{dir})}(p_{K^-}, p_{\Xi^-})/dp_{\Xi^-}}{A d\sigma_{K^-C \rightarrow \Xi^-X}^{(\text{dir})}(p_{K^-}, p_{\Xi^-})/dp_{\Xi^-}}. \quad (28)$$

We define now the total inelastic Ξ^-p and Ξ^-n cross sections $\sigma_{\Xi^-p}^{\text{in}}$ and $\sigma_{\Xi^-n}^{\text{in}}$, appearing in Eq. (17) and used in our calculations of Ξ^- production in K^-A reactions. At Ξ^- momenta below 1 GeV/c of interest these cross sections are entirely exhausted by the total cross sections $\sigma_{\Xi^-p \rightarrow \Lambda\Lambda}$, $\sigma_{\Xi^-p \rightarrow \Xi^0 n}$, $\sigma_{\Xi^-p \rightarrow \Lambda\Sigma^0}$ and $\sigma_{\Xi^-n \rightarrow \Lambda\Sigma^-}$ of the processes $\Xi^-p \rightarrow \Lambda\Lambda$, $\Xi^-p \rightarrow \Xi^0 n$, $\Xi^-p \rightarrow \Lambda\Sigma^0$ and $\Xi^-n \rightarrow \Lambda\Sigma^-$. While the first two channels are open at any finite Ξ^- momentum in free scattering, the last two inelastic ones open only at momenta of about 0.57 and 0.59 GeV/c, respectively, in this scattering. At considered Ξ^- momenta we can ignore the processes $\Xi^-p \rightarrow \Lambda\Lambda\pi^0$, $\Xi^-N \rightarrow \Lambda\Sigma\pi$ and $\Xi^-N \rightarrow \Sigma\Sigma$, since they only open at threshold momenta around 1 GeV/c. Thus, these momenta

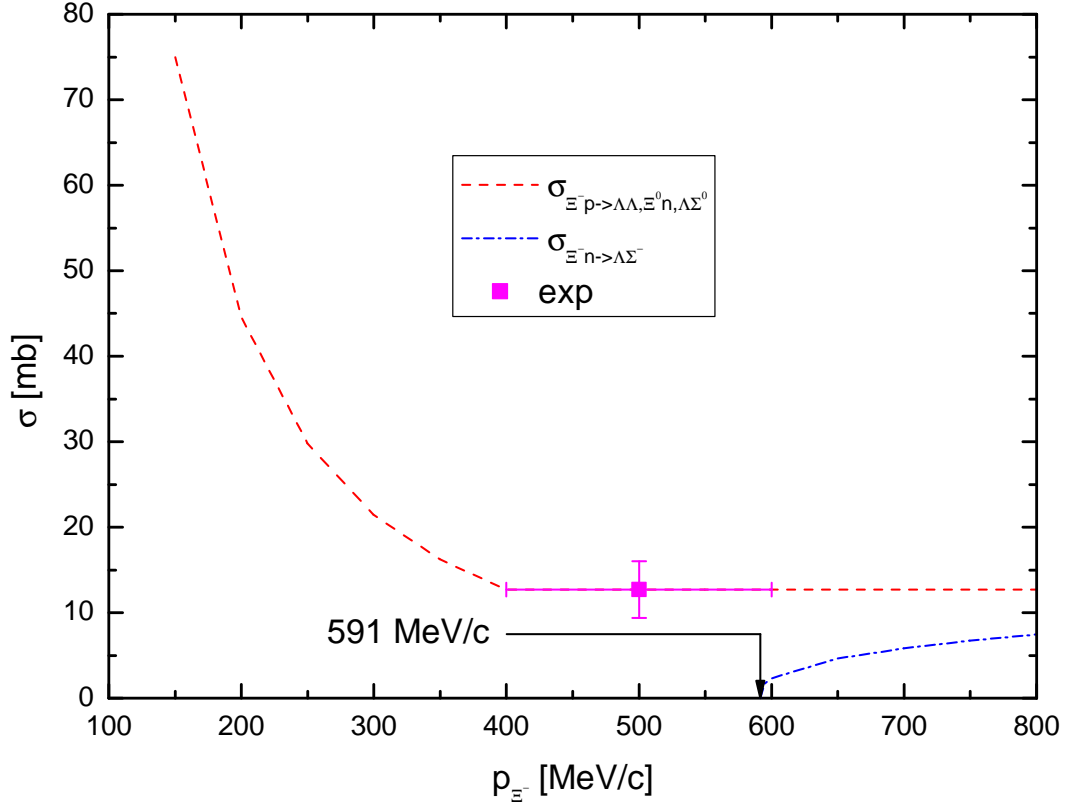


Figure 4: (Color online) Ξ^- hyperon momentum dependence of the total cross sections for the reactions $\Xi^- p \rightarrow \Lambda\Lambda, \Xi^0 n, \Lambda\Sigma^0$ and $\Xi^- n \rightarrow \Lambda\Sigma^-$. The arrow indicates the free threshold momentum for the latter one. For the rest of the notation see the text.

in free $\Xi^- N$ interactions are about 0.87, 1.20 and 0.96 GeV/c, respectively. With these, we have

$$\sigma_{\Xi^- p}^{\text{in}} = \sigma_{\Xi^- p \rightarrow \Lambda\Lambda, \Xi^0 n, \Lambda\Sigma^0} = \sigma_{\Xi^- p \rightarrow \Lambda\Lambda} + \sigma_{\Xi^- p \rightarrow \Xi^0 n} + \sigma_{\Xi^- p \rightarrow \Lambda\Sigma^0}, \quad (29)$$

$$\sigma_{\Xi^- n}^{\text{in}} = \sigma_{\Xi^- n \rightarrow \Lambda\Sigma^-}. \quad (30)$$

The cross section $\sigma_{\Xi^- p \rightarrow \Lambda\Lambda, \Xi^0 n, \Lambda\Sigma^0}$ was calculated in [88] at laboratory Ξ^- momenta ≤ 800 MeV/c within the updated version chiral EFT at the NLO for ΞN interaction, which is in line with the empirical information on the $\Lambda\Lambda$ S -wave scattering length [89] and fulfills all available scarce experimental constraints [100, 101, 109, 110, 111] on the $\Xi^- p$ elastic and inelastic cross sections and leads to a weakly attractive single-particle potential of the Ξ^- hyperon in nuclear matter as evidenced by recent observation of the existence of Ξ^- hypernuclei (see above). We parametrize the results of calculations [88] by the following laboratory Ξ^- momentum p_{Ξ^-} dependence:

$$\sigma_{\Xi^- p}^{\text{in}}(p_{\Xi^-}) = \sigma_{\Xi^- p \rightarrow \Lambda\Lambda, \Xi^0 n, \Lambda\Sigma^0}(p_{\Xi^-}) = \begin{cases} 2.417/(p_{\Xi^-})^{1.8106} \text{ [mb]} & \text{for } 0.15 \leq p_{\Xi^-} \leq 0.4 \text{ GeV/c,} \\ 12.7 \text{ [mb]} & \text{for } 0.4 < p_{\Xi^-} \leq 0.8 \text{ GeV/c,} \end{cases} \quad (31)$$

where momentum p_{Ξ^-} is expressed in GeV/c. For illustration this dependence is shown in Fig. 4 by the dashed curve. As visible in Fig. 4, it fits well the available data point taken from [110] over

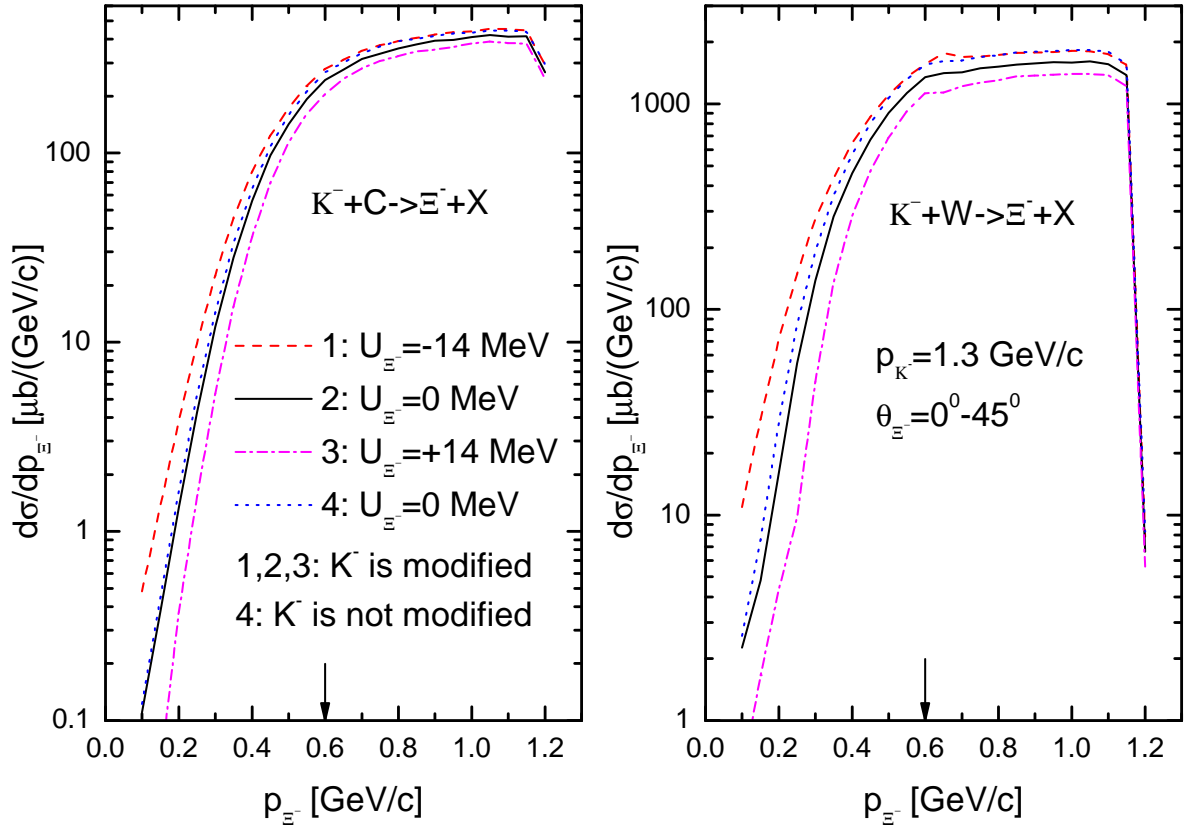


Figure 5: (Color online) Momentum differential cross sections for the production of Ξ^- hyperons from the direct $K^-p \rightarrow K^+\Xi^-$ and $K^-n \rightarrow K^0\Xi^-$ processes in the laboratory polar angular range of $0^\circ-45^\circ$ in the interaction of medium-modified and not modified K^- mesons having vacuum momentum of 1.3 GeV/c with ^{12}C (left) and ^{184}W (right) nuclei, calculated for different values of the Ξ^- hyperon effective scalar potential U_{Ξ^-} at density ρ_0 indicated in the inset and for the nominal Ξ^- absorption in the nuclear matter. The arrows indicate the boundary between the low-momentum and high-momentum parts of the Ξ^- spectra.

the momentum range $400 < p_{\Xi^-} < 600$ MeV/c. The on-shell cross section of $\Xi^0 p \rightarrow \Lambda\Sigma^+$ (or due to the isospin symmetry of $\Xi^- n \rightarrow \Lambda\Sigma^-$) reaction, calculated within the previous version chiral EFT at the NLO [89], was parametrized by us as follows:

$$\sigma_{\Xi^- n}^{\text{in}}(p_{\Xi^-}) = \sigma_{\Xi^- n \rightarrow \Lambda\Sigma^-}(p_{\Xi^-}) = 23.448 \left(\sqrt{s_{\Xi^-}(p_{\Xi^-})} - \sqrt{s_0} \right)^{0.353} \text{ [mb]}, \quad (32)$$

where

$$s_{\Xi^-}(p_{\Xi^-}) = (E_{\Xi^-} + m_N)^2 - p_{\Xi^-}^2 \quad (33)$$

and $\sqrt{s_0} = m_\Lambda + m_{\Sigma^-} = 2.313132$ GeV is the free threshold energy for the $\Xi^- n \rightarrow \Lambda\Sigma^-$ reaction. For completeness, this parametrization is shown in Fig. 4 by the dotted-dashed curve. For the in-medium $\Xi^- p$ and $\Xi^- n$ inelastic cross sections we use Eqs. (31) and (32), in which one needs to make only the substitution $p_{\Xi^-} \rightarrow p'_{\Xi^-}$. Following the predictions of the approaches [85, 86, 87, 112, 113] that the Λ and Σ hyperons experience only a moderately attractive and repulsive potentials $\sim -(10-20)$ MeV and $+(10-20)$ MeV, respectively, at central densities and relevant Λ and

Σ finite momenta \sim , as showed our estimates, 300 MeV/c, we assume that the threshold energy $\sqrt{s_0}$ entering into Eq. (32) is not changed in the nuclear medium due to cancellation of these potentials. To study the sensitivity of the Ξ^- hyperon production cross sections from processes (1) and (2) to its absorption in nuclear matter we will also employ in our calculations yet two additional scenarios for the Ξ^-p and Ξ^-n nominal inelastic cross sections (31) and (32), in which these cross sections were artificially multiplied by factors $f = 0.5$ and $f = 2$.

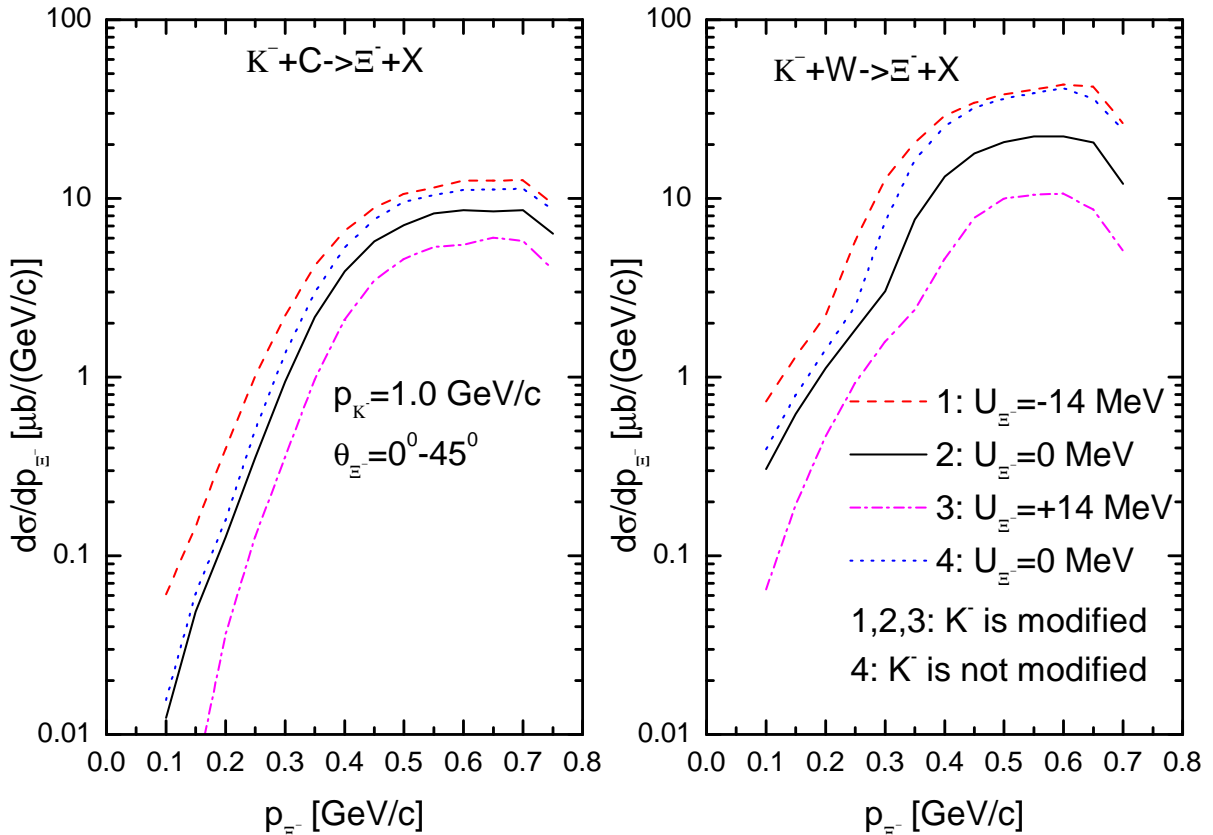


Figure 6: (Color online) The same as in Fig. 5, but for the initial vacuum antikaon momentum of 1.0 GeV/c.

3 Results and discussion

At first, we consider the momentum dependences of the absolute Ξ^- hyperon differential cross sections from the direct production processes (1) and (2) in $K^{-12}\text{C}$ and $K^{-184}\text{W}$ interactions. They were calculated on the basis of Eq. (27) for three basic adopted values of the Ξ^- effective scalar potential U_{Ξ^-} at density ρ_0 for laboratory angles of 0° – 45° and for initial vacuum antikaon momenta of 1.3 and 1.0 GeV/c. Also the nominal absorption of Ξ^- hyperons in the nuclear matter was accounted for. These dependences are depicted, respectively, in Figs. 5 and 6. It is seen from these figures that the Ξ^- hyperon differential cross sections reveal a certain sensitivity to this potential, mostly in the low-momentum region of 0.1–0.6 GeV/c, for both target nuclei and for both considered antikaon momenta. Here, the differences between calculations corresponding to different

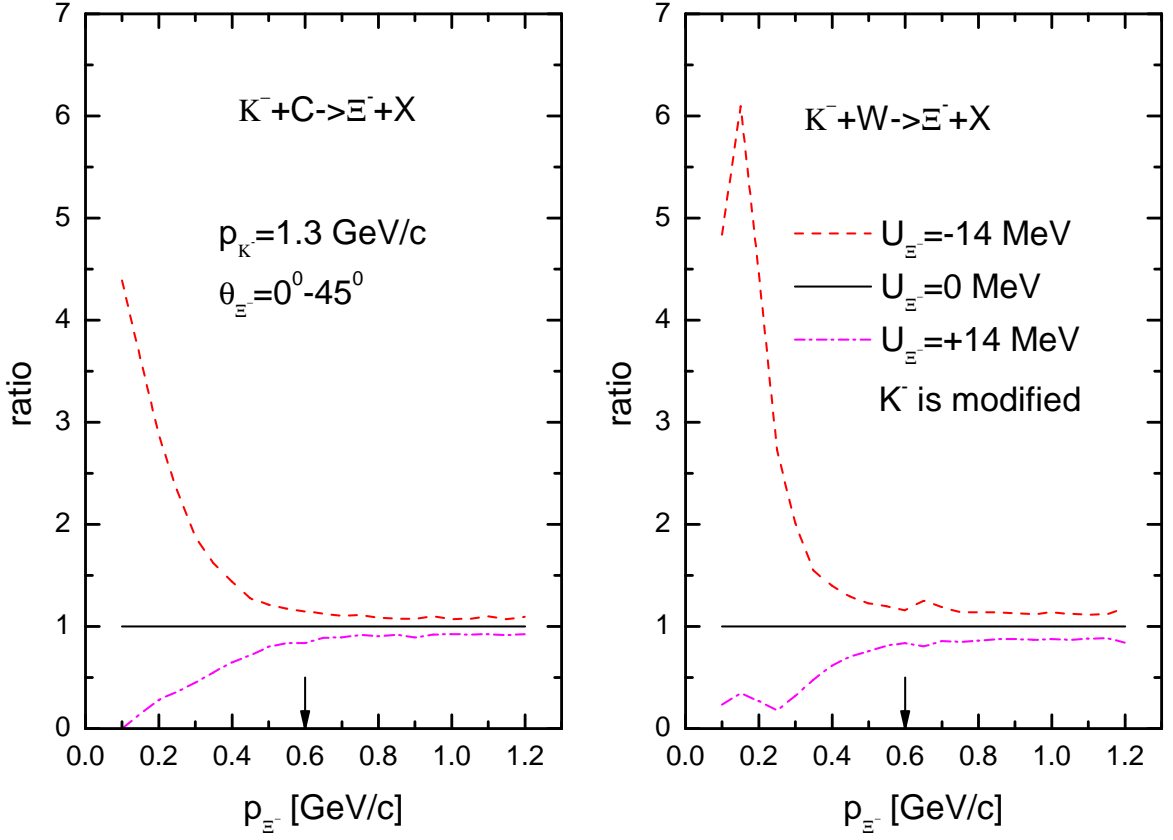


Figure 7: (Color online) Ratio between the differential cross sections for Ξ^- production on ^{12}C (left) and ^{184}W (right) target nuclei in the angular region of 0° – 45° by medium-modified K^- mesons having vacuum momentum of 1.3 GeV/c, calculated with and without the Ξ^- hyperon in-medium mass shift U_{Ξ^-} at density ρ_0 indicated in the inset and for the nominal Ξ^- absorption in the nuclear matter, as a function of Ξ^- momentum. The arrows indicate the boundary between the low-momentum and high-momentum parts of the Ξ^- spectra.

choices for the Ξ^- scalar potential U_{Ξ^-} are well separated and experimentally distinguishable. They are practically similar to each other for each target nucleus at initial antikaon momenta considered. Thus, for example, for incident vacuum K^- meson momentum of 1.3 GeV/c and for outgoing Ξ^- hyperon momenta of 0.2, 0.4, 0.6 GeV/c the inclusion of the Ξ^- attractive potential of -14 MeV at normal nuclear matter density leads in the case of ^{12}C nucleus to an enhancement of the Ξ^- production cross sections by factors of about 2.9, 1.4, 1.2, respectively, as compared to those obtained for the potential $U_{\Xi^-} = 0$ MeV. In the case of ^{184}W target nucleus these enhancement factors are about 4.5, 1.4, 1.2. At initial vacuum K^- momentum of 1.0 GeV/c and the same outgoing hyperon momenta of 0.2, 0.4, 0.6 GeV/c the corresponding enhancement factors are similar and are about 3.1, 1.7, 1.5 and 2.0, 2.2, 2.0 in the cases of ^{12}C and ^{184}W target nuclei, correspondingly. On the other hand, the inclusion of the Ξ^- repulsive potential of +14 MeV at density ρ_0 results in the reduction of the Ξ^- hyperon production cross sections by factors of about 3.5, 1.5, 1.2 and 3.7, 1.6, 1.2 compared to those calculated at zero Ξ^- potential for incoming vacuum antikaon momentum of 1.3 GeV/c and for the same outgoing vacuum Ξ^- momenta of 0.2, 0.4, 0.6 GeV/c in the cases of ^{12}C and ^{184}W target nuclei, respectively. And for incident beam momentum of 1.0 GeV/c and for the

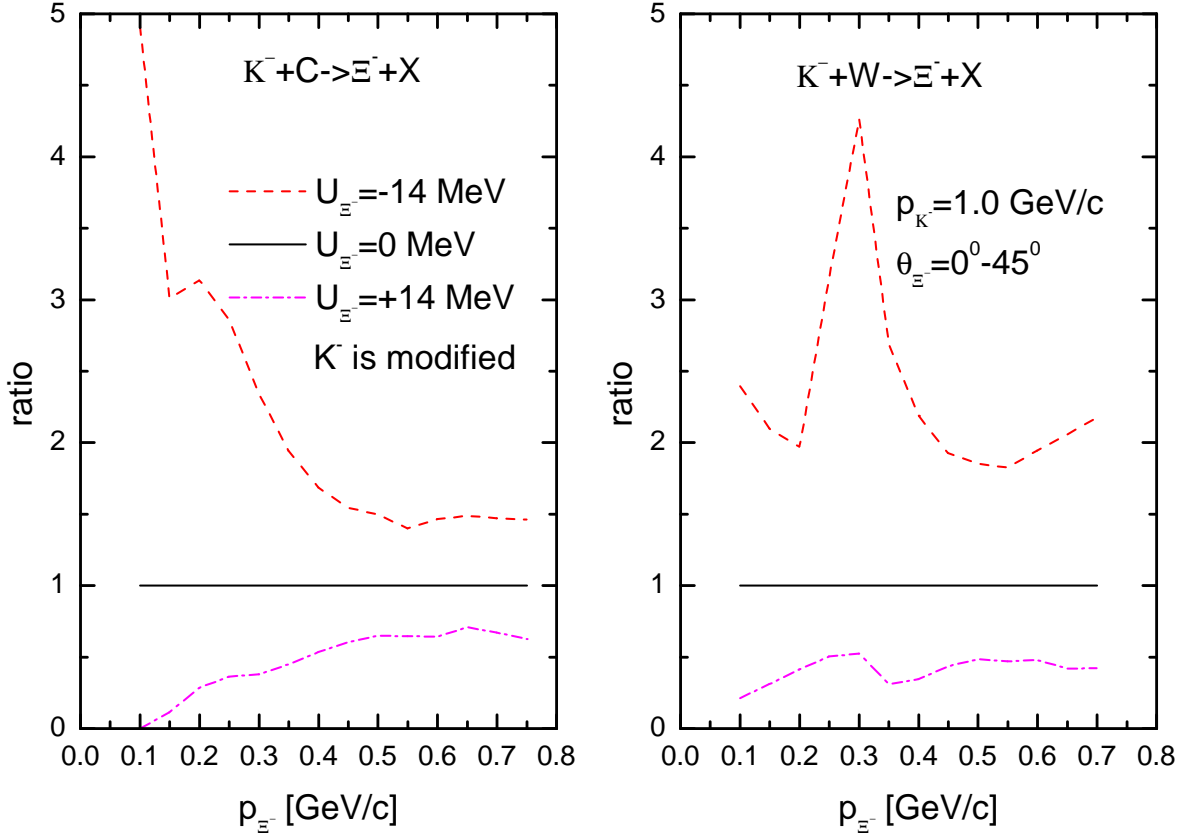


Figure 8: (Color online) The same as in Fig. 7, but for the initial vacuum antikaon momentum of 1.0 GeV/c.

same final Ξ^- momenta these reduction factors are similar and are about 3.5, 1.9, 1.6 and 2.4, 2.9, 2.1 for ^{12}C and ^{184}W , correspondingly. However, although the Ξ^- hyperon production differential cross sections at beam momentum of 1.0 GeV/c are less than those at the momentum of 1.3 GeV/c by about of one to two orders of magnitude their strength at the former momentum is still large enough to be measured in the present experimental facilities. Thus, the Ξ^- hyperon differential cross sections measurements in the near-threshold incident K^- momentum region (at 1.0–1.3 GeV/c) will open a possibility to shed light on its nuclear potential in cold nuclear matter. Such measurements could be performed in the future at the J-PARC Hadron Experimental Facility using the high-intensity separated secondary K^- beams. The calculations considered above have been carried out, supposing that the incoming vacuum K^- meson momentum is modified in the interior of the nucleus in line with Eqs. (3), (10), (11) due to the presence here of the nuclear attractive optical potential U_{K^-} and the Coulomb potential V_{cK^-} . In order to study the sensitivity of the cascade hyperon production cross sections from the one-step processes (1), (2) to these potentials, we have used in our calculations also zero values for them. The results of such calculations for Ξ^- potential $U_{\Xi^-} = 0$ MeV at saturation density ρ_0 are presented in Figs. 5 and 6 by the dotted curves. One can see that the influence of the antikaon–nucleon strong and electromagnetic interactions on the free Ξ^- production is negligible at incident vacuum K^- momentum of 1.3 GeV/c, but favorable for the lower incoming momentum of 1.0 GeV/c. The latter gives us the need to account for these interactions in our subsequent calculations.

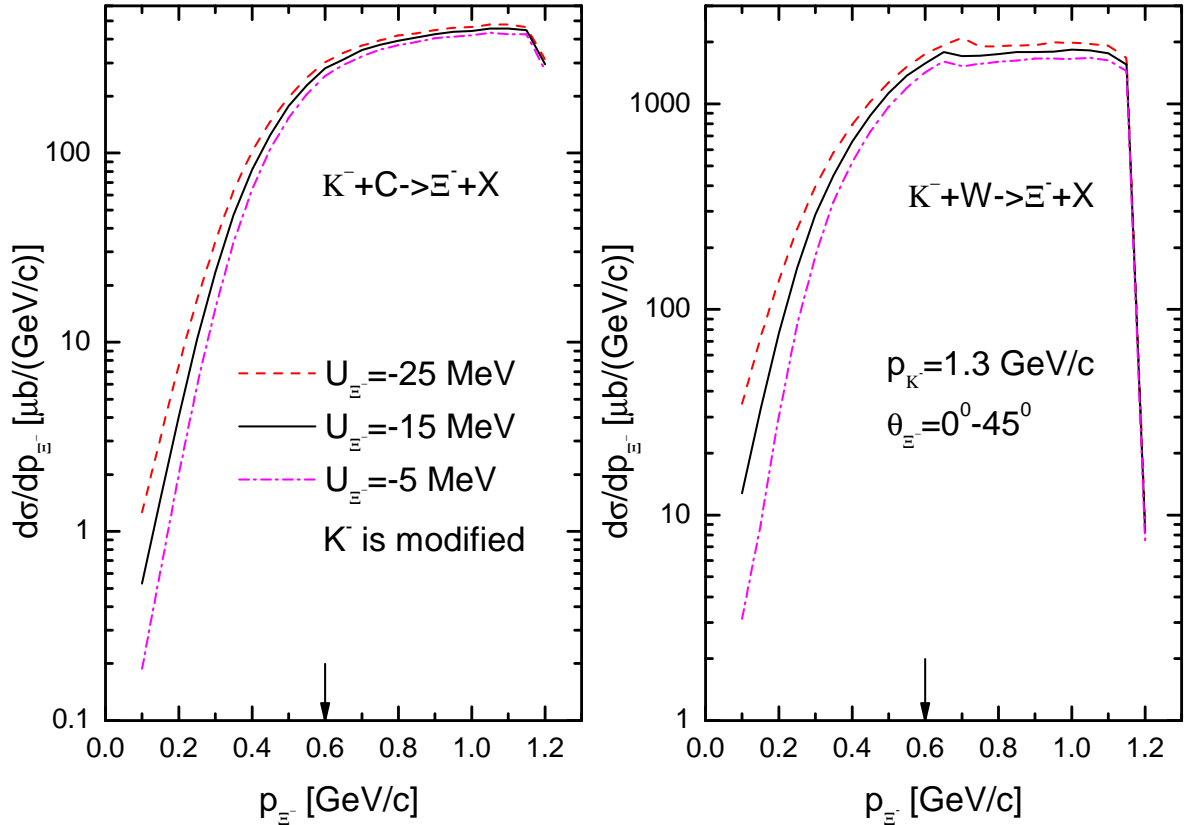


Figure 9: (Color online) Momentum differential cross sections for the production of Ξ^- hyperons from the direct $K^-p \rightarrow K^+\Xi^-$ and $K^-n \rightarrow K^0\Xi^-$ processes in the laboratory polar angular range of 0° – 45° in the interaction of medium-modified K^- mesons having vacuum momentum of 1.3 GeV/c with ^{12}C (left) and ^{184}W (right) nuclei, calculated for another compared to the above different values of the Ξ^- hyperon effective scalar potential U_{Ξ^-} at density ρ_0 indicated in the inset and for the nominal Ξ^- absorption in the nuclear matter. The arrows indicate the boundary between the low-momentum and high-momentum parts of the Ξ^- spectra.

To see more clearly the sensitivity of the differential cross sections, presented in Figs. 5 and 6, to the Ξ^- hyperon scalar potential U_{Ξ^-} at the central density ρ_0 , we show in Figs. 7 and 8 the momentum dependences of the ratios of these cross sections, calculated for the Ξ^- potential U_{Ξ^-} , to the analogous cross section, determined at $U_{\Xi^-} = 0$ MeV, on a linear scale for ^{12}C and ^{184}W nuclei at incident vacuum K^- momenta of 1.3 and 1.0 GeV/c, respectively. It should be noted that such relative observables are more favorable compared to those based on the absolute cross sections for the aim of getting the information on particle nuclear potential, since the theoretical uncertainties associated with the particle production and absorption mechanisms essentially cancel out in them. It is clearly seen from Fig. 7 that at the incident vacuum K^- meson momentum of 1.3 GeV/c there are indeed experimentally distinguishable differences at the Ξ^- hyperon momenta ≤ 0.6 GeV/c between the results corresponding to the considered options for its scalar potential U_{Ξ^-} for both target nuclei. At initial subthreshold antikaon momentum of 1.0 GeV/c such differences exist for these nuclei, as follows from Fig. 8, in the whole Ξ^- momentum range studied – at momenta both below and above 0.6 GeV/c. This means that the in-medium properties of Ξ^- hyperons could be

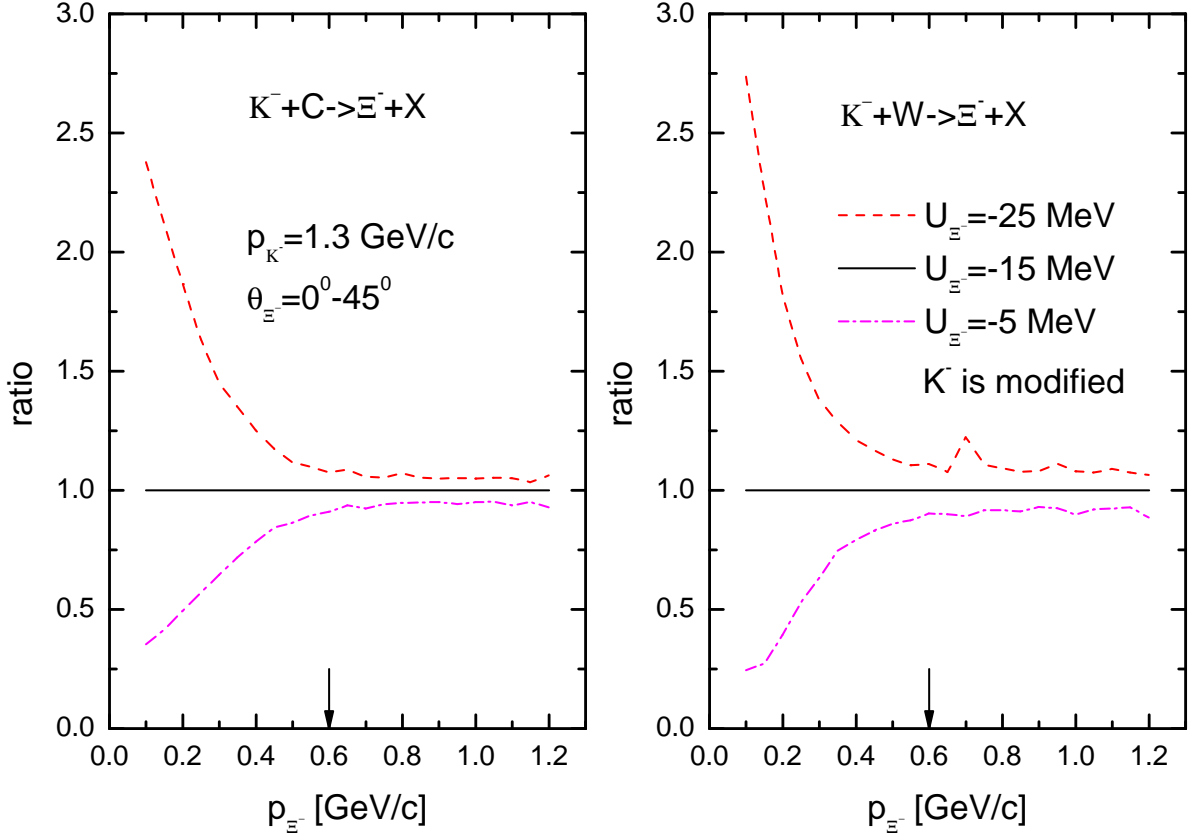


Figure 10: (Color online) Ratio between the differential cross sections for Ξ^- production on ^{12}C (left) and ^{184}W (right) target nuclei in the angular region of 0° – 45° by medium-modified K^- mesons having vacuum momentum of 1.3 GeV/c, calculated with the Ξ^- hyperon in-medium mass shift U_{Ξ^-} at density ρ_0 indicated in the inset and with the shift $U_{\Xi^-} = -15$ MeV for the nominal Ξ^- absorption in the nuclear matter, as a function of Ξ^- momentum. The arrows indicate the boundary between the low-momentum and high-momentum parts of the Ξ^- spectra.

investigated at J-PARC, using K1.8 or K1.8BR beamlines, through the momentum dependence of their absolute (and relative) production cross sections in inclusive K^-A reactions at initial K^- momenta ~ 1.0 – 1.3 GeV/c. It should be pointed out that the ratios of differential cross sections for Ξ^- hyperon production on ^{184}W nucleus by 1.0 GeV/c antikaons, presented in Fig. 8, are peaked at Ξ^- momentum ~ 0.3 GeV/c for adopted values of ± 14 MeV for its scalar potential U_{Ξ^-} at density ρ_0 . This can be explained by the fact that the Ξ^- production cross section, determined at zero value of this potential, ”is bent down” at momenta around this momentum (see Fig. 6) due to the off-shell kinematics of the direct K^-N collisions and the role played by the nucleus-related effects such as the target proton binding and Fermi motion, encoded in the nuclear spectral function $P_A(\mathbf{p}_t, E)$. The spectral functions for nuclei ^{12}C and ^{184}W , employed in the present work, are different [75, 103, 104].

For completeness, in Figs. 9 and 10 we show, respectively, the Ξ^- differential cross sections and their ratios, analogous to those presented in Figs. 5 and 7, but calculated for the three additional low-energy Ξ^- potential values of (-25,-15,-5) MeV at density ρ_0 . It is seen that and in this case the low-momentum (0.1–0.6 GeV/c) region reveals a definite sensitivity to the Ξ^- potential, which

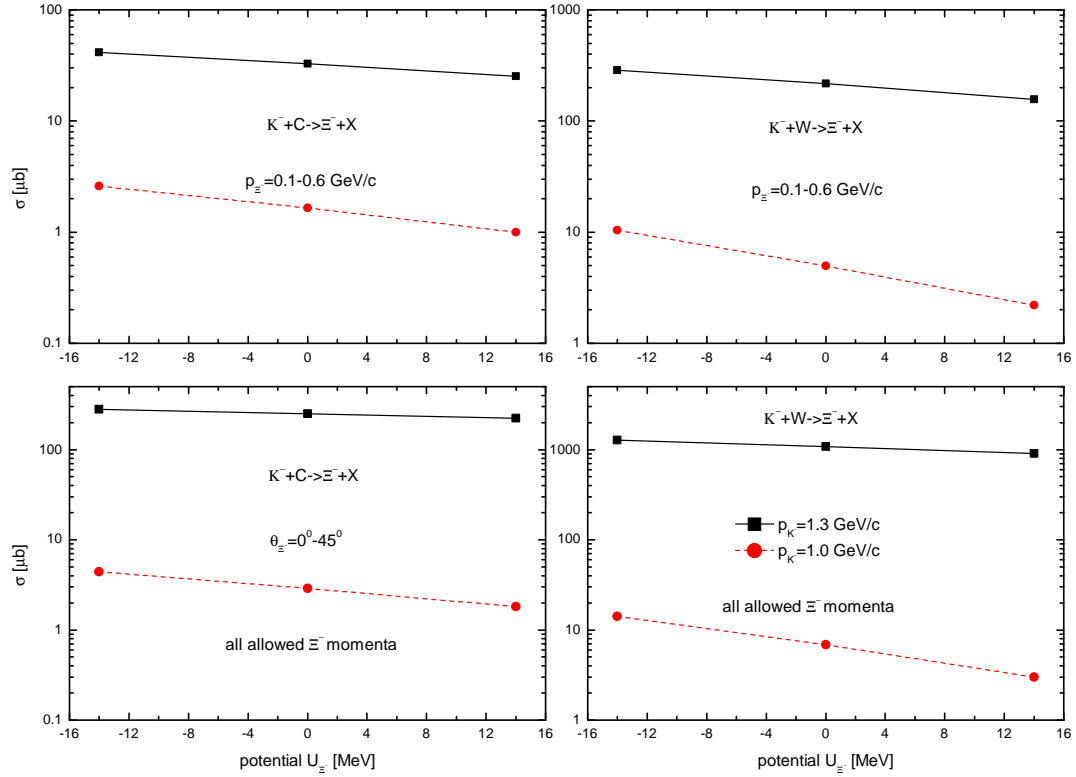


Figure 11: (Color online) Total cross sections for the production of Ξ^- hyperons from the direct $K^-p \rightarrow K^+\Xi^-$ and $K^-n \rightarrow K^0\Xi^-$ processes on ^{12}C and ^{184}W nuclei with momenta of 0.1–0.6 GeV/c (upper two panels) and with all allowed Ξ^- momenta ≥ 0.1 GeV/c at given vacuum incident beam momentum (lower two panels) in the laboratory polar angular range of 0° – 45° by medium-modified K^- mesons having vacuum momenta of 1.0 and 1.3 GeV/c, calculated for the nominal Ξ^- absorption in the nuclear matter, as functions of the effective scalar Ξ^- potential U_{Ξ^-} at normal nuclear density. The lines are visual guides.

can be exploited to discriminate experimentally between also these low-energy scenarios for the in-medium Ξ^- hyperon modification.

The sensitivity of the Ξ^- hyperon production differential cross sections to its effective scalar potential U_{Ξ^-} , demonstrated in Figs. 5, 6 and 7, 8, can also be studied from such integral measurements as the measurements of the total cross sections for Ξ^- production in $K^-^{12}\text{C}$ and $K^-^{184}\text{W}$ interactions at laboratory angles $\leq 45^\circ$ for the near-threshold incident K^- momenta of 1.0 and 1.3 GeV/c. Such total cross sections, calculated by integrating Eq. (27) over the Ξ^- momentum p_{Ξ^-} in the low-momentum region (0.1–0.6 GeV/c) and in the full-momentum region allowed for the given beam momentum are shown in Fig. 11 as functions of this potential. It can be seen that the low-momentum region of 0.1–0.6 GeV/c shows higher sensitivity to the potential U_{Ξ^-} than the full-momentum one. Thus, for instance, the ratios between the total cross sections for Ξ^- hyperon production by 1.0, 1.3 GeV/c K^- mesons on ^{12}C and ^{184}W nuclei in this momentum region, calculated with the potential $U_{\Xi^-} = -14$ MeV, and the cross sections, obtained with $U_{\Xi^-} = +14$ MeV, are about 2.6, 1.6 and 4.7, 1.8, respectively. Whereas the same ratios in the full-momentum regions

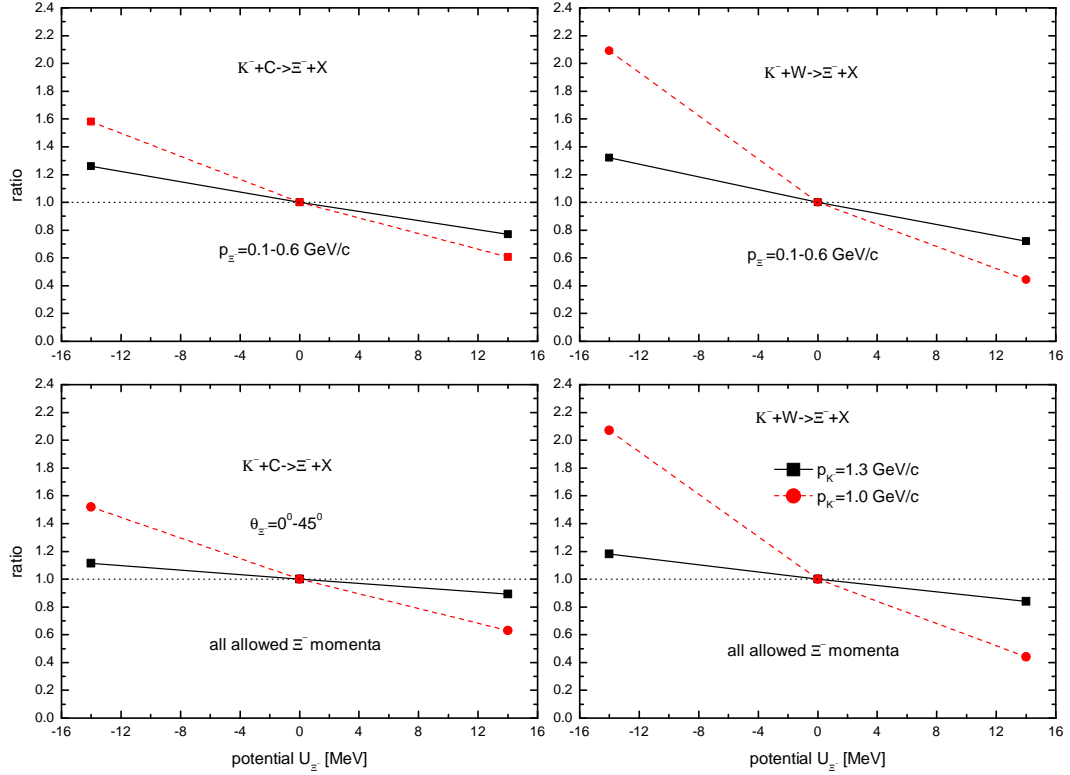


Figure 12: (Color online) Ratio between the total cross sections for the production of Ξ^- hyperons from the direct $K^-p \rightarrow K^+\Xi^-$ and $K^-n \rightarrow K^0\Xi^-$ processes on ^{12}C and ^{184}W nuclei at laboratory angles of 0° – 45° with momenta of 0.1–0.6 GeV/c (upper two panels) and with all allowed Ξ^- momenta ≥ 0.1 GeV/c at given vacuum incident beam momentum (lower two panels) by medium-modified K^- mesons having vacuum momenta of 1.0 and 1.3 GeV/c, calculated for the nominal Ξ^- absorption in the nuclear matter with and without the Ξ^- effective scalar potential U_{Ξ^-} at normal nuclear density, as function of this potential. The lines are visual guides.

are only somewhat smaller: they are about 2.4, 1.3 for ^{12}C and 4.7, 1.4 for ^{184}W , correspondingly. The highest sensitivity of the total cross sections for Ξ^- production in the low-momentum and in the full-momentum regions to the potential U_{Ξ^-} is observed at K^- momentum of 1.0 GeV/c. Despite the fact that the cross sections at this momentum are smaller than those at beam momentum of 1.3 GeV/c by about of one – two orders of magnitude, they have a measurable strength ~ 1 – $10 \mu\text{b}$. Therefore, the total cross section measurements of Ξ^- hyperon production on nuclei both in the low-momentum (0.1–0.6 GeV/c) and in the full-momentum regions for incident antikaon momenta not far below and above threshold (for momenta ~ 1.0 – 1.3 GeV/c) will also allow to shed light on its in-medium properties.

Fig. 12 shows the results, which also support the findings of Fig. 11 that the total Ξ^- hyperon production cross sections both in the low-momentum (0.1–0.6 GeV/c) and in the full-momentum regions reveal a some sensitivity to its in-medium scalar potential U_{Ξ^-} at saturation density ρ_0 for the considered incident K^- momenta. Here, the ratios of the Ξ^- production total cross sections, calculated for the potential U_{Ξ^-} and presented in Fig. 11, to the analogous cross sections, determined

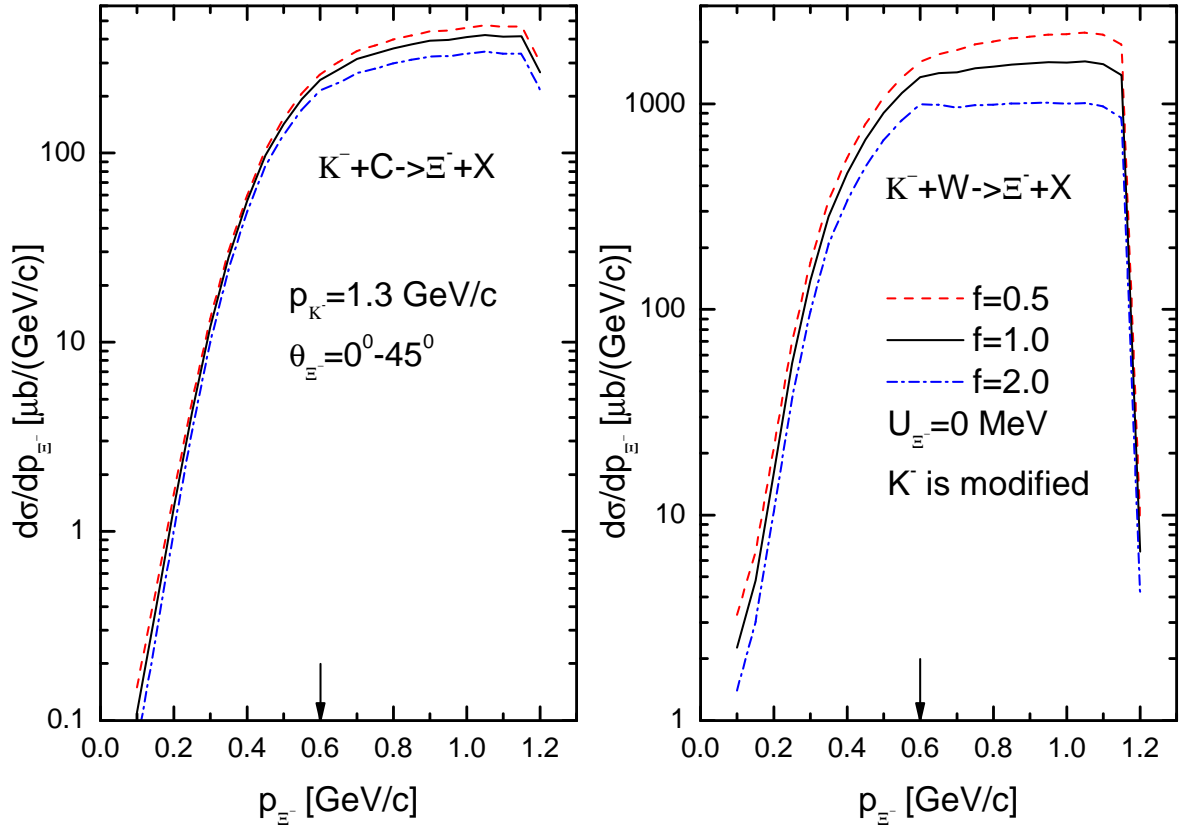


Figure 13: (Color online) Momentum differential cross sections for the production of Ξ^- hyperons from the direct $K^-p \rightarrow K^+\Xi^-$ and $K^-n \rightarrow K^0\Xi^-$ processes in the laboratory polar angular range of 0° – 45° in the interaction of medium-modified K^- mesons having vacuum momentum of 1.3 GeV/c with ^{12}C (left) and ^{184}W (right) nuclei, calculated for value of the Ξ^- hyperon effective scalar potential $U_{\Xi^-} = 0$ MeV at density ρ_0 assuming that its total inelastic cross section $\sigma_{\Xi^-N}^{\text{in}}$ is multiplied by the factors indicated in the inset. The arrows indicate the boundary between the low-momentum and high-momentum parts of the Ξ^- spectra.

at $U_{\Xi^-} = 0$ MeV, are shown as functions of this potential. It is nicely seen that the highest sensitivity of the ratios in both considered kinematic regions to the potential U_{Ξ^-} is indeed observed at subthreshold K^- momentum of 1.0 GeV/c. Thus, at this momentum and for these regions the cross section ratios for $U_{\Xi^-} = -14$ MeV are about 1.5 and 2.1 for ^{12}C and ^{184}W targets, respectively. As the antikaon momentum increases to 1.3 GeV/c, the sensitivity of the total cross section ratios to variations in the Ξ^- hyperon effective scalar potential U_{Ξ^-} decreases. Thus, in the case where Ξ^- hyperons of momenta of 0.1–0.6 GeV/c are produced by 1.3 GeV/c K^- mesons impinging on ^{12}C and ^{184}W nuclei, the considered ratios for $U_{\Xi^-} = -14$ MeV take smaller but yet a measurable values of about 1.3 and 1.3, respectively. The analogous ratios for the production of the Ξ^- hyperons in the full-momentum regions by 1.3 GeV/c antikaons in ^{12}C and ^{184}W target nuclei are yet smaller: they are ~ 1.1 and 1.2, respectively.

To study the sensitivity of the Ξ^- hyperon production cross sections to its absorption cross section in nuclear medium in near-threshold antikaon-induced reactions, we calculated the absolute Ξ^- momentum differential cross sections from the direct processes (1) and (2) in $K^-^{12}\text{C}$ and $K^-^{184}\text{W}$

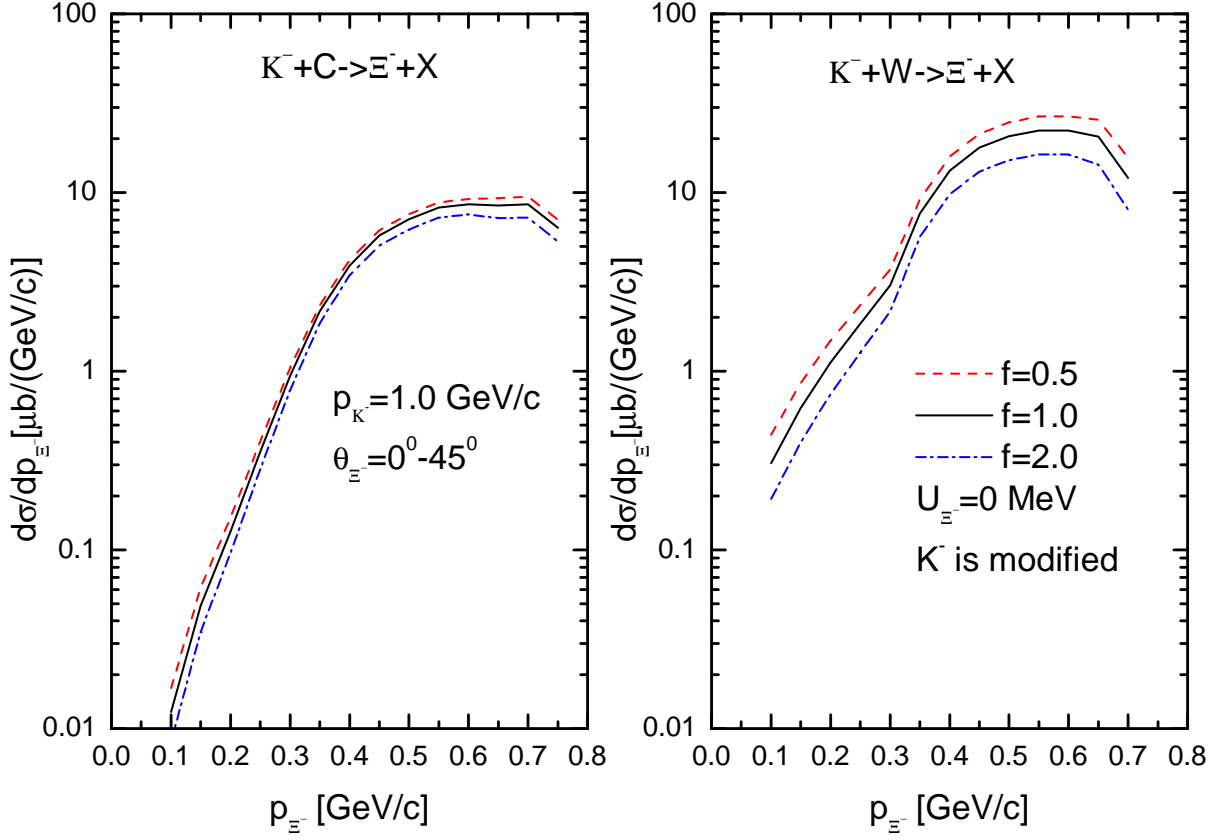


Figure 14: (Color online) The same as in Fig. 13, but for the initial vacuum antikaon momentum of 1.0 GeV/c.

collisions for an incident vacuum K^- momenta of 1.3 and 1.0 GeV/c at laboratory angles $\leq 45^\circ$ for zero value of its potential U_{Ξ^-} at density ρ_0 assuming that Ξ^-N nominal inelastic cross section, given by Eqs. (17), (31) and (32), is multiplied by the factor $f = 0.5, 1.0, 2.0$. They are shown in Figs. 13 and 14, respectively. It is seen from Fig. 13 that there are a sizeable differences ($\sim 10\text{--}20\%$ for ^{12}C and $\sim 20\text{--}40\%$ for ^{184}W) between all calculations corresponding to different considered choices for the Ξ^-N inelastic cross section. While these differences are comparable in the high-momentum range of 0.6–1.2 GeV/c (where the Ξ^- production cross sections are the greatest) with those caused by the modification of the Ξ^- hyperon mass in nuclear matter due to the strong interaction, they are significantly less than the latter ones at momenta below 0.6 GeV/c (cf. Fig. 5), where the role of the Ξ^- scalar potential is essential. At initial Ξ^- momentum of 1.0 GeV/c the latter differences are significantly larger, as follows from Figs. 6 and 14, than the former ones at all final Ξ^- momenta. This leads to the important conclusion that a comparison of the "differential" and "integral" results depicted in Figs. 5–12 with the corresponding experimental data, which could be taken in the dedicated experiment at J-PARC, should allow one to distinguish at least between zero, possible weak attractive ($U_{\Xi^-} \sim -14$ MeV) and weak repulsive ($U_{\Xi^-} \sim +14$ MeV) Ξ^- hyperon scalar potentials in cold nuclear matter in spite of the fact that the Ξ^-N inelastic cross section is experimentally unknown at low Ξ^- momenta.

Finally, it is also interesting to clarify additionally the opportunity of extracting the strength of the Ξ^- hyperon effective scalar potential at saturation density ρ_0 from the measurements of such

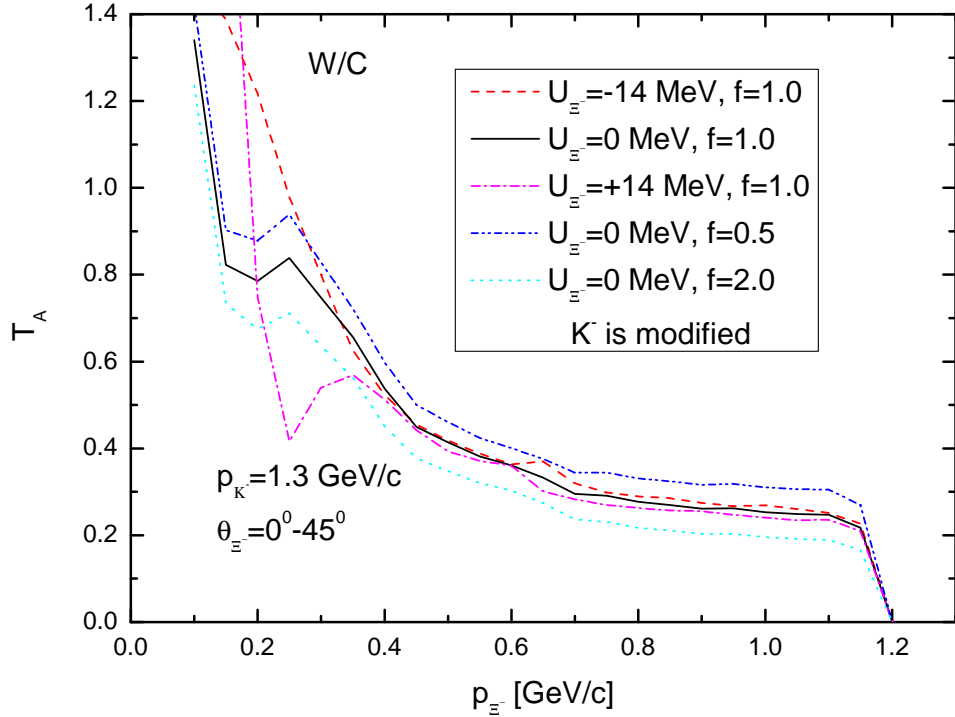


Figure 15: (Color online) Transparency ratio T_A as a function of the Ξ^- hyperon momentum for combination $^{184}\text{W}/^{12}\text{C}$ as well as for the Ξ^- laboratory polar angular range of 0° – 45° , for an incident vacuum K^- meson momentum of 1.3 GeV/c and for different values of its effective scalar potential U_{Ξ^-} at density ρ_0 and of the factor f indicated in the inset.

relative observable as the transparency ratio T_A for Ξ^- hyperons, as this has been done for the η' and J/ψ mesons in Refs. [114] and [115], respectively. Figures 15 and 16 show the momentum dependence of this quantity for the W/C combination for Ξ^- hyperons produced in the primary channels (1) and (2) at laboratory angles $\leq 45^\circ$ by 1.3 and 1.0 GeV/c antikaons, respectively. It is calculated according to Eq. (28) for the adopted values of the Ξ^- hyperon effective scalar potential U_{Ξ^-} at density ρ_0 and of the factor f , by which its total inelastic cross section is multiplied. One can see that for the subthreshold K^- meson momentum of 1.0 GeV/c there is, contrary to the case of its above threshold momentum of 1.3 GeV/c, a strong sensitivity (~ 40 – 60%) of the transparency ratio T_A to the considered variations in the nuclear potential U_{Ξ^-} at all outgoing Ξ^- momenta, which cannot be practically masked by that (~ 10 – 20%) associated with the possible changes in the Ξ^-N inelastic cross section. This means that the future precise Ξ^- production data on the momentum dependence of the transparency ratio T_A for Ξ^- hyperons, taken for the initial antikaon momentum of 1.0 GeV/c, should also help, with accounting for the results given in Figs. 15 and 16, to determine the Ξ^- hyperon effective scalar potential in cold nuclear matter at its density ρ_0 .

Thus, taking into account the above considerations, one can conclude that the Ξ^- differential and total cross section measurements in antikaon–nucleus reactions at initial momenta not far from threshold (at momenta ~ 1.0 – 1.3 GeV/c) as well as the transparency ratio measurements for Ξ^- hyperons at subthreshold momenta ~ 1.0 GeV/c will allow us to shed light on this potential.

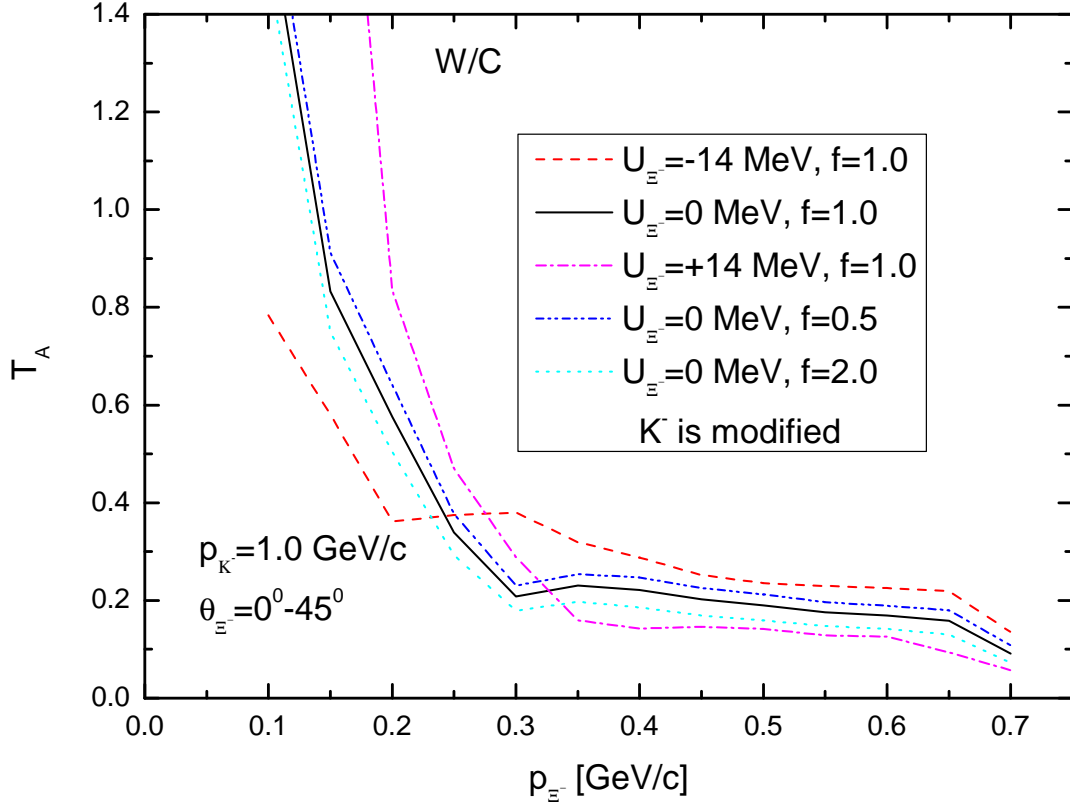


Figure 16: (Color online) The same as in Fig. 15, but for the initial vacuum antikaon momentum of 1.0 GeV/c.

4 Summary

In the present paper we study the antikaon-induced inclusive cascade Ξ^- hyperon production from ^{12}C and ^{184}W target nuclei near threshold within a nuclear spectral function approach. The approach describes incoherent direct Ξ^- hyperon production in elementary $K^-p \rightarrow K^+\Xi^-$ and $K^-n \rightarrow K^0\Xi^-$ processes as well as takes into account the influence of the scalar nuclear K^-, K^+, K^0, Ξ^- and their Coulomb potentials on these processes. We calculate the absolute differential and total cross sections for the production of Ξ^- hyperons off these nuclei at laboratory angles $\leq 45^\circ$ by K^- mesons with momenta of 1.0 and 1.3 GeV/c, which are close to the threshold momentum (1.05 GeV/c) for Ξ^- hyperon production on the free target nucleon at rest. We also calculate the momentum dependence of the transparency ratio for the $^{184}\text{W}/^{12}\text{C}$ combination for Ξ^- hyperons at these K^- beam momenta. We show that the Ξ^- differential and total (absolute and relative) production cross sections at the considered initial momenta reveal a distinct sensitivity to the variations in the scalar Ξ^- nuclear potential at saturation density ρ_0 , studied in the paper, in the low-momentum region of 0.1–0.6 GeV/c. We also demonstrate that for the subthreshold K^- meson momentum of 1.0 GeV/c there is, contrary to the case of its above threshold momentum of 1.3 GeV/c, a strong sensitivity of the transparency ratio for Ξ^- hyperons to the considered changes in the Ξ^- nuclear potential at all outgoing Ξ^- momenta as well, which cannot be masked, as in the case of differential and total observables mentioned above, by that associated with the possible changes in the poorly

known experimentally $\Xi^- N$ inelastic cross section. Therefore, the measurement of these absolute and relative observables in a dedicated experiment at the J-PARC Hadron Experimental Facility will provide valuable information on the Ξ^- in-medium properties, which will be complementary to that deduced from the study of the inclusive (K^-, K^+) reactions at incident momenta of 1.6–1.8 GeV/c in the Ξ^- bound and quasi-free regions.

References

- [1] W. Cassing and E. L. Bratkovskaya, Phys. Rep. **308**, 65 (1999).
C. Fuchs, Prog. Part. Nucl. Phys. **56**, 1 (2006);
arXiv:nucl-th/0507017.
C. Hartnack *et al.*, Phys. Rep. **510**, 119 (2012);
arXiv:1106.2083 [nucl-th].
O. Buss *et al.*, Phys. Rep. **512**, 1 (2012);
arXiv:1106.1344 [hep-ph].
- [2] E. Friedman and A. Gal, Phys. Rep. **452**, 89 (2007);
arXiv:0705.3965 [nucl-th].
- [3] L. Tolos and L. Fabbietti, Prog. Part. Nucl. Phys. **112**, 103770 (2020);
arXiv:2002.09223 [nucl-ex].
- [4] L. Tolos, R. Molina, E. Oset, and A. Ramos, Phys. Rev. C **82**, 045210 (2010);
arXiv:1006.3454 [nucl-th].
- [5] E. Oset *et al.*, Int. J. Mod. Phys. E **21**, 1230011 (2012);
arXiv:1210.3738 [nucl-th].
- [6] A. Ilner, D. Cabrera, P. Srisawad, and E. Bratkovskaya, Nucl. Phys. A **927**, 249 (2014);
arXiv:1312.5215 [hep-ph].
- [7] D. Cabrera *et al.*, Journal of Physics: Conf. Series **503**, 012017 (2014);
arXiv:1312.4343 [hep-ph].
L. Tolos, EPJ Web of Conf. **171**, 09003 (2018).
- [8] K. Tsushima, A. Sibirtsev, and A. W. Thomas, Phys. Rev. C **62**, 064904 (2000);
arXiv:nucl-th/0004011.
- [9] D. Suenaga and P. Lakaschus, Phys. Rev. C **101**, 035209 (2020);
arXiv:1908.10509 [nucl-th].
- [10] E. Ya. Paryev, Chinese Physics C, Vol. **44**, No. (11), 114106 (2020);
arXiv:2007.10192 [nucl-th].
- [11] S. H. Lee and S. Cho, Int. J. Mod. Phys. E **22**, 1330008 (2013);
arXiv:1302.0642 [nucl-th].
- [12] T. Song, T. Hatsuda, and S. H. Lee, Phys. Lett. B **792**, 160 (2019);
arXiv:1808.05372 [nucl-th].
- [13] S. H. Lee, arXiv:1904.09064 [nucl-th].

- [14] S. H. Lee, Nucl. Part. Phys. Proc. **309–311**, 111 (2020).
- [15] E. Ya. Paryev, Nucl. Phys. A **1007**, 122133 (2021);
arXiv:2102.00789 [nucl-th].
- [16] M. M. Kaskulov and E. Oset, Phys. Rev. C **73**, 045213 (2006);
arXiv:nucl-th/0509088.
- [17] M. M. Kaskulov and E. Oset, AIP Conf. Proc. **842**, 483–5 (2006).
- [18] M. F. M. Lutz, C. L. Copra and M. Moeller, Nucl. Phys. A **808**, 124 (2008);
arXiv:0707.1283 [nucl-th].
- [19] D. Cabrera *et al.*, Phys. Rev. C **90**, 055207 (2014);
arXiv:1406.2570 [hep-ph].
- [20] S. Petschauer *et al.*, arXiv:2002.00424 [nucl-th].
- [21] Z. Q. Feng, W. J. Xie, and G. M. Jin, Phys. Rev. C **90**, 064604 (2014).
- [22] E. Ya. Paryev and Yu. T. Kiselev, Nucl. Phys. A **992**, 121622 (2019);
arXiv:1910.02755 [nucl-th].
- [23] M. Kaskulov, L. Roca and E. Oset, Eur. Phys. J. A **28**, 139 (2006);
arXiv:nucl-th/0601074.
- [24] E. Ya. Paryev, Phys. Atom. Nucl. Vol. **75**, No.12, 1523 (2012).
- [25] E. Ya. Paryev, J. Phys. G: Nucl. Part. Phys. **37**, 105101 (2010);
arXiv:1010.0111 [nucl-th].
- [26] A. Gal, E. V. Hungerford and D. J. Millener, Rev. Mod. Phys. **88**, 035004 (2016);
arXiv:1605.00557 [nucl-th].
- [27] T. Hatsuda *et al.*, Nucl. Phys. A **967**, 856 (2017);
arXiv:1704.05225 [nucl-th].
- [28] K. Sasaki *et al.* (HAL QCD Collaboration), Nucl. Phys. A **998**, 121737 (2020);
arXiv:1912.08630 [hep-lat].
K. Sasaki *et al.* (HAL QCD Collaboration), EPJ Web Conf. **175**, 05010 (2018).
- [29] C. B. Dover and A. Gal, Annals of Phys. **146**, 309 (1983).
- [30] S. Aoki *et al.*, Phys. Lett. B **355**, 45 (1995).
- [31] T. Fukuda *et al.*, Phys. Rev. C **58**, 1306 (1998).
- [32] P. Khaustov *et al.*, Phys. Rev. C **61**, 054603 (2000);
arXiv:nucl-ex/9912007.
- [33] T. Iijima *et al.*, Nucl. Phys. A **546**, 588 (1992).
- [34] T. Nagae *et al.* (J-PARC E05 Collaboration), PoS INPC **2016**, 038 (2017);
AIP Conf. Proc. **2130**, 020015 (2019).
- [35] H. Maekawa *et al.*, arXiv:0704.3929 [nucl-th].

- [36] H. Maekawa, K. Tsubakihara and A. Ohnishi, Eur. Phys. J. A **33**, 269 (2007); arXiv:nucl-th/0701066.
- [37] J. Hu and H. Shen, Phys. Rev. C **96**, 054304 (2017); arXiv:1710.08613 [nucl-th].
- [38] E. Hiyama *et al.*, Phys. Rev. C **78**, 054316 (2008); arXiv:0811.3156 [nucl-th].
- [39] Y. Jin, X.-R. Zhou, Yi-Yu. Cheng and H.-J. Schulze, arXiv:1910.05884 [nucl-th].
- [40] T. Miyatsu and K. Saito, Prog. Theor. Phys. **122**, 1035 (2009); arXiv:0903.1893 [nucl-th].
- [41] M. Kohno and Y. Fujiwara, Phys. Rev. C **79**, 054318 (2009); arXiv:0904.0517 [nucl-th].
- [42] K. Nakazawa *et al.*, Prog. Theor. Exp. Phys. **2015**, 033D02 (2015).
- [43] S. H. Hayakawa *et al.* (J-PARC E07 Collaboration), Phys. Rev. Lett. **126**, 062501 (2021); arXiv:2010.14317 [nucl-ex].
- [44] M. Yoshimoto *et al.*, arXiv:2103.08793 [nucl-ex].
- [45] E. Hiyama *et al.*, Phys. Rev. Lett. **124**, 092501 (2020); arXiv:1910.02864 [nucl-th].
- [46] G. Meher and U. Raha, arXiv:2010.12291 [nucl-th].
- [47] Md. A. Khan *et al.*, arXiv:2011.03708 [nucl-th].
- [48] H. Ohnishi, F. Sakuma, and T. Takahashi, arXiv:1912.02380 [nucl-ex].
- [49] B. Abelev *et al.* (ALICE Collaboration), Phys. Lett. B **728**, 216 (2014); arXiv:1307.5543 [nucl-ex].
- [50] J. Castillo (STAR Collaboration), Nucl. Phys. A **715**, 518 (2003); arXiv:nucl-ex/0210032.
- [51] J. Adams *et al.* (STAR Collaboration), Phys. Rev. Lett. **98**, 062301 (2007); arXiv:nucl-ex/0606014.
- [52] M. M. Aggarwal *et al.* (STAR Collaboration), Phys. Rev. C **83**, 024901 (2011); arXiv:1010.0142 [nucl-ex].
- [53] S. V. Afanasiev *et al.* (NA49 Collaboration), Phys. Lett. B **538**, 275 (2002); arXiv:hep-ex/0202037.
- [54] F. Antinori *et al.* (NA57 Collaboration), Phys. Lett. B **595**, 68 (2004).
F. Antinori *et al.* (NA57 Collaboration), J. Phys. G **31**, 1345 (2005); arXiv:nucl-ex/0509009.
- [55] C. Alt *et al.* (NA49 Collaboration), Phys. Rev. C **78**, 034918 (2008); arXiv:0804.3770 [nucl-ex].
- [56] P. Chung *et al.* (E895 Collaboration), Phys. Rev. Lett. **91**, 202301 (2003); arXiv:nucl-ex/0302021.

- [57] G. Agakishiev *et al.* (HADES Collaboration), Phys. Rev. Lett. **103**, 132301 (2009); arXiv:0907.3582 [nucl-ex].
- [58] A. Andronic, P. Braun-Munzinger, and K. Redlich, Nucl. Phys. A **765**, 211 (2006).
- [59] L.-W. Chen, C. M. Ko, and Y. Tzeng, Phys. Lett. B **584**, 269 (2004); arXiv:nucl-th/0312009.
- [60] F. Li, L.-W. Chen, C. M. Ko and S. H. Lee, Phys. Rev. C **85**, 064902 (2012); arXiv:1204.1327 [nucl-th].
- [61] G. Graef *et al.*, Phys. Rev. C **90**, 064909 (2014); arXiv:1409.7954 [nucl-th].
- [62] A. Aduszkiewicz *et al.* (NA61/SHINE Collaboration), arXiv:2006.02062 [nucl-ex].
- [63] F. Antinori *et al.* (NA57 Collaboration), J. Phys. G **32**, 427 (2006); arXiv:nucl-ex/0601021.
- [64] G. Agakishiev *et al.* (HADES Collaboration), Phys. Rev. Lett. **114**, 212301 (2015); arXiv:1501.03894 [nucl-ex].
- [65] J. W. Price *et al.* (CLAS Collaboration), Nucl. Phys. A **754**, 272c (2005); arXiv:nucl-ex/0402006.
- [66] J. W. Price *et al.* (CLAS Collaboration), Phys. Rev. C **71**, 058201 (2005); arXiv:nucl-ex/0409030.
- [67] L. Guo *et al.* (CLAS Collaboration), Phys. Rev. C **76**, 025208 (2007); arXiv:nucl-ex/0702027.
- [68] G. Barucca *et al.* (PANDA Collaboration), arXiv:2009.11582 [hep-ex]; arXiv:2012.01776 [hep-ex]; arXiv:2101.11877 [hep-ex].
- [69] J. Adamczewski-Musch *et al.* (HADES Collaboration with PANDA@HADES Collaboration), arXiv:2010.06961 [nucl-ex].
- [70] Y. Nara *et al.*, Nucl. Phys. A **614**, 433 (1997).
- [71] E. Ya. Paryev, Chinese Physics C, Vol. **42**, No. (8), 084101 (2018); arXiv:1806.00303 [nucl-th].
- [72] E. Ya. Paryev, M. Hartmann and Yu. T. Kiselev, J. Phys. G: Nucl. Part. Phys. **42**, 075107 (2015); arXiv:1505.01992 [nucl-th].
- [73] E. Ya. Paryev, Eur. Phys. J. A **23**, 453 (2005).
- [74] M. Kohno, Phys. Rev. C **100**, 024313 (2019); arXiv:1908.01934 [nucl-th].
- [75] E. Ya. Paryev, Eur. Phys. J. A **9**, 521 (2000).
- [76] V. Metag, M. Nanova, and E. Ya. Paryev, Prog. Part. Nucl. Phys. **97**, 199 (2017); arXiv:1706.09654 [nucl-ex].
- [77] K. Tsushima *et al.*, Phys. Lett. B **429**, 239 (1998).

- [78] E. Ya. Paryev, M. Hartmann and Yu. T. Kiselev, *Chinese Physics C*, Vol.**41**, No.12, 124108 (2017); arXiv:1612.02767 [nucl-th].
- [79] A. Sibirtsev and W. Cassing, *Nucl. Phys. A* **641**, 476 (1998); arXiv:nucl-th/9805021.
- [80] G. Q. Li and C. M. Ko, *Phys. Rev. C* **54**, 1897 (1996); arXiv:nucl-th/9608049.
- [81] Z. Q. Feng, *Phys. Rev. C* **101**, 064601 (2020); arXiv:2006.02247 [nucl-th].
- [82] C.-H. Lee *et al.*, *Phys. Lett. B* **412**, 235 (1997); arXiv:nucl-th/9705012.
- [83] C. B. Dover and G. E. Walker, *Phys. Rep.* **89**, 1 (1982).
- [84] N.-Y. Ghim *et al.*, arXiv:2102.05292 [nucl-th].
- [85] T. Gaitanos and A. Choroziadou, arXiv:2101.08470 [nucl-th].
- [86] T. Inoue (for HAL QCD Collaboration), *AIP Conf. Proc.* **2130**, no.1, 020002 (2019); arXiv:1809.08932 [hep-lat].
- [87] T. Inoue (for HAL QCD Collaboration), *PoS INPC 2016*, 277 (2016); arXiv:1612.08399 [hep-lat].
- [88] J. Haidenbauer and U.- G. Meissner, *Eur. Phys. J. A* **55**, 23 (2019); arXiv:1810.04883 [nucl-th].
- [89] J. Haidenbauer, U.- G. Meissner, and S. Petschauer, *Nucl. Phys. A* **954**, 273 (2016); arXiv:1511.05859 [nucl-th].
- [90] M. M. Nagels, Th. A. Rijken, and Y. Yamamoto, arXiv:1504.02634 [nucl-th].
- [91] M. Kohno, *Phys. Rev. C* **81**, 014003 (2010); arXiv:0912.4330 [nucl-th].
- [92] H. Polinder, J. Haidenbauer, and U.-G. Meissner, *Phys. Lett. B* **653**, 29 (2007); arXiv:0705.3753 [nucl-th].
- [93] M. Nanova *et al.* (CBELSA/TAPS Collaboration), *Phys. Lett. B* **727**, 417 (2013); arXiv:1311.0122 [nucl-ex].
- [94] M. Nanova *et al.* (CBELSA/TAPS Collaboration), *Phys. Rev. C* **94**, 025205 (2016); arXiv:1607.07228 [nucl-ex].
- [95] T. Harada and Y. Hirabayashi, *Phys. Rev. C* **103**, 024605 (2021); arXiv:2101.00855 [nucl-th].
- [96] E. E. Kolomeitsev, B. Tomasik, and D. N. Voskresensky, *Phys. Rev. C* **86**, 054909 (2012); arXiv:1207.5738 [nucl-th].
- [97] B. Tomasik and E. E. Kolomeitsev, arXiv:1510.04349 [nucl-th].
- [98] T. Harada and Y. Hirabayashi, *Phys. Rev. C* **102**, 024618 (2020); arXiv:2006.15627 [nucl-th].
- [99] E. Friedman and A. Gal, arXiv:2104.00421 [nucl-th].
- [100] T. Tamagawa *et al.*, *Nucl. Phys. A* **691**, 234c (2001).

- [101] J. K. Ahn *et al.*, Phys. Lett. B **633**, 214 (2006);
arXiv:nucl-ex/0502010.
- [102] J. K. Ahn and S.-il Nam, arXiv:2101.10114 [hep-ph].
- [103] S. V. Efremov and E. Ya. Paryev, Eur. Phys. J. A **1**, 99 (1998).
- [104] E. Ya. Paryev, Eur. Phys. J. A **7**, 127 (2000).
- [105] A. Sibirtsev *et al.*, Z. Phys. A **351**, 333 (1995).
- [106] A. Sibirtsev and W. Cassing, arXiv:nucl-th/9909053.
- [107] V. Flaminio *et al.*, Compilation of Cross Sections.
II: K^+ and K^- Induced Reactions. CERN-HERA **83-02**, (1983).
- [108] D. A. Sharov, V. L. Korotkikh, and D. E. Lanskoj, Eur. Phys. J. A **47**, 109 (2011);
arXiv:1105.0764 [nucl-th].
- [109] J. K. Ahn *et al.*, Nucl. Phys. A **625**, 231 (1997).
- [110] S. Aoki *et al.*, Nucl. Phys. A **644**, 365 (1998).
- [111] S. J. Kim *et al.*, presentation at the 12th Int. Conf. on Hypernuclear and
Strange Particle Physics. Sendai, Japan (2015);
<http://lambda.phys.tohoku.ac.jp/hyp2015/>
- [112] J. Haidenbauer and U.- G. Meissner, Nucl. Phys. A **936**, 29 (2015);
arXiv:1411.3114 [nucl-th].
- [113] S. Petschauer *et al.*, Eur. Phys. J. A **52**, 15 (2016);
arXiv:1507.08808 [nucl-th].
- [114] E. Ya. Paryev, J. Phys. G: Nucl. Part. Phys. **40**, 025201 (2013);
arXiv:1209.4050 [nucl-th].
- [115] E. Ya. Paryev, Yu. T. Kiselev, and Yu. M. Zaitsev, Nucl. Phys. A **968**, 1 (2017).